Abstract

Inhibitor of Apoptosis Proteins (IAPs) are negative regulators of apoptosis and their overexpression is observed in many cancer cells, correlating with the inhibition of caspases. IAPs inhibitory function is exploited by the BIR domains, which were firstly identified in baculovirus. Among the IAP family, XIAP (X chromosome-linked IAP) directly inhibits caspases preventing proteolytic cleavage through its BIR2 and BIR3 domains; furthermore, XIAP-BIR1 in a dimeric form recognizes TAB1, a kinase activator, regulating pro-survival pathways. In the last years, cIAPs have become crucial players of the extrinsic pathway; in fact, through the recognition of TRAFs (TNF Receptor Associated Factors) by the cIAP2-BIR1 domain, they are recruited to the TNF-α Receptor Signaling Complex and act as E3 ubiquitin ligases. One of the most promising approaches that have been proposed to inhibit these proteins is represented by the structure-based design of small molecules, named Smac-mimetics, that mimic Smac/DIABLO (Second mitochondria-derived activator of caspases/Direct IAp Binding protein with Low pI), an endogenous antagonist of IAPs. Initially designed in 2001 against the BIR3 domain of XIAP, Smac-mimetics have shown to prevent the inhibitory action of XIAP on initiator and executioner caspases, but also to bind to the BIR3 of cIAPs, inducing their autoubiquitylation and degradation. This work focuses on the cloning, expression and purification of the IAPs constructs of interest and their biochemical and biophysical characterization alone and in the presence of some of the Smac-mimetics from our library. The X-ray technique on crystals and protein solutions allowed a structural study of the protein-ligand complexes at atomic level, favoring the process of drug lead optimization. Furthermore, the screening of libraries of pharmacologically active compounds through *in silico* docking searches on new targets, such as XIAP- and cIAP2-BIR1, resulted in the discovery of potential new pro-apoptotic leads, whose clinical properties are known. Since in the last months new macromolecular protein complexes have been identified as involved in apoptosis and pro-survival pathways, novel protocols for the expression and purification of cIAP1 and TRAFs full length constructs have been optimized to obtain pure and homogeneous samples ready for the structural characterization.

State of the art

How IAPs are involved in apoptosis

Eukaryotes maintain cellular homeostasis by a process of programmed cell death, named apoptosis [1], which is regulated by a subset of caspases (Cysteine-dependent ASPartyl-specific proteASES) in charge of perpetuating, once activated, the apoptotic signal to the nucleus. Caspases activation and its prevention are subject to very tight control by many cellular factors. For instance, members of the Bcl-2 family work upstream to integrate cellular signals that positively or negatively regulate caspases, without a direct association to them[2]. A direct suppression of caspases activity occurs in the presence of specific members of the IAP (Inhibitor of Apoptosis Proteins) family [3; 4], such as XIAP (X-chromosome-linked IAP), whereas cIAP1 and cIAP2 (cellular IAPs) are indirect inhibitors. These proteins have been extensively investigated in the last few years, and proposed as drug targets, since they are known to be abnormally regulated and expressed at high levels in the majority of human malignancies [5]. IAPs inhibitory function is exploited by the BIR (Baculoviral IAP Repeat) domains, which are highly conserved in several organisms and were firstly identified in baculovirus (figure 1, panel A). IAPs contain one to three BIRs, which are usually composed of five α-helices (α1-2 at the N terminus, and α3-5 at the C-terminus), and a three-stranded β-sheet, hosting a Zinc-finger motif, that however is not endowed with DNA-binding activity. IAPs also contain an Ubiquitin-associated (UBA) domain, which enables the binding of polyubiquitin conjugates [6; 7; 8] and a RING (Really Interesting New Gene) domain, that exploits the E3-ubiquitin ligase activity upon dimerization. A Caspase Activation and Recruitment Domain (CARD) is present only in some IAPs (cIAPs),

where it is necessary for autoregulation, preventing RING dimerization, E2 binding and E2 activation [9] (figure 1, panel B).

Among the IAP family, XIAP is one of the most characterized members of the intrinsic (or mitochondrial) apoptotic pathway at a structural and functional level. Although XIAP-null mice are viable, it was recently shown that loss of XIAP function causes elevated caspase 3 activity [8]. In fact, structural and biochemical evidences show that XIAP directly inhibits effector caspases 3, 7 and initiator caspase 9 preventing proteolytic cleavage through its BIR2 and BIR3 domains, respectively [10; 11; 12]. Furthermore, XIAP-BIR1 in a dimeric form recognizes TAB1 (TAK Binding protein 1), a kinase activator, promoting the NF-κB survival pathway. This can apparently occur by a structural mechanism proposed by Lu *et al.* where BIR1- and RING- mediated dimerization of XIAP allows the recognition and dimerization of TAB1 and subsequent dimerization and activation of TAK1 and NF-κB [13]. Finally, recent studies report that the RING domain of XIAP controls cancer cell motility, and therefore malignant cancer progression, being involved in the β-actin polymerization and cytoskeleton formation [14]. However, the precise role of XIAP in the determination of cancer biological behavior remains unclear.

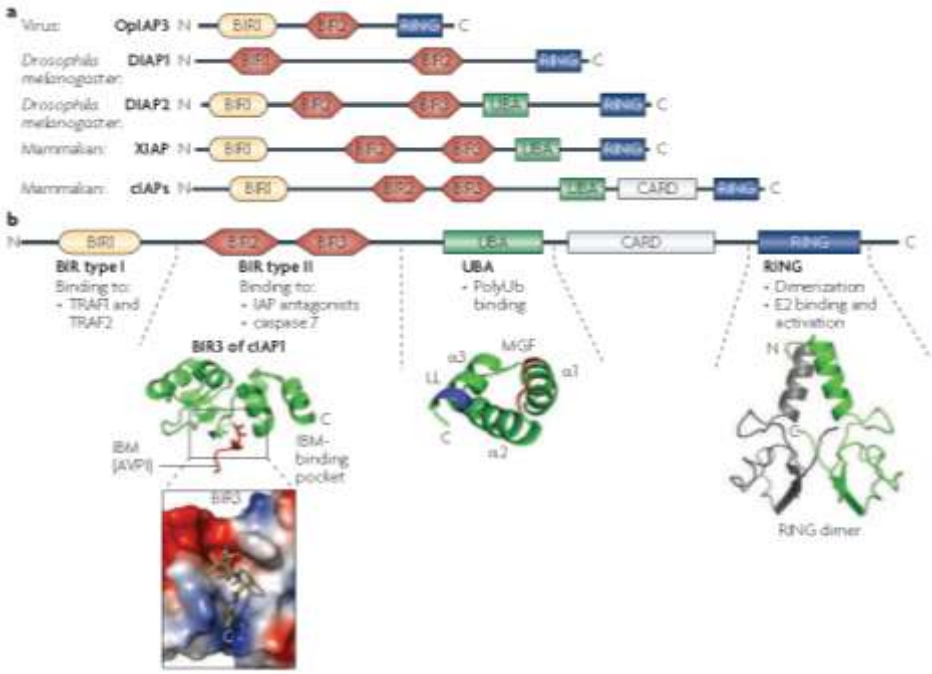

Figure 1. A The first inhibitor of apoptosis (IAP) protein, OpIAP, was identified from a baculovirus strain in 1993 by Miller and colleagues[15], on the basis of its ability to suppress virus-induced apoptosis of infected cells. Cellular IAPs were subsequently identified in insects and vertebrates. In mammalian IAPs, baculovirus IAP repeat (BIR) domains enable interactions with proteins. The BIR domains of IAPs can be grouped into type I (yellow) and type II (red) BIR domains on the basis of the presence or absence of a deep peptide-binding groove. **B** Proteins such as caspases and IAP antagonists interact with type II BIR domains, whereas tumour necrosis factor receptor-associated factor 1 (TRAF1) and TRAF2 interact with type I BIR domains. The structure of the cIAP1-BIR3 peptide-binding groove bound to the amino-terminal portion of the IAP antagonist Smac is shown (AVPI; red). The UBA domain binds polyubiquitin (polyUb) and its structure is known by NMR[16]. The amino acid residues MGF and LL (shown in red and blue, respectively) of the UBA domain form the hydrophobic interaction surface that mediates binding to polyUb chains. The caspase-recruitment domain (CARD), which generally serves as a protein interaction surface, is required for cIAP1 autoregulation. The carboxy-terminal RING domain is required for Ub ligase activity, and is a dimerization interface and docking site for ubiquitin conjugating enzymes (E2s). The structure of a cIAP2 RING dimer is shown; the grey and green structures depict two respective cIAP2 molecules[17].

In the last years, many laboratories focused on cIAP1 and cIAP2 as crucial players of the extrinsic pathway, being recruited to the TNF-α Receptor

Signaling Complex, acting in an eterodimeric form as E3 ligases and ubiquitylating substrates [18]. In detail, elongated proteins named TRAFs (TNF Receptor Associated Factors) function as platforms for the recruitment of cIAPs to TNF-RSC, recognizing specific residues of the cIAP2-BIR1 domain. This binding event is essential for cIAPs activity [19], which consists of the ubiquitylation of substrates involved in the canonical and non-canonical NF-κB pathways, where cIAPs positively or negatively regulate the survival of the cell. In the first case (figure 2, on the left), upon stimulation with TNF-α, TNFR1 recruits the adaptor protein TRADD, which in turn recruits TRAF2 and RIP1. RIP1 becomes modified with K63-linked polyubiquitin chains by cIAP1/2 for downstream NF-κB activation. In the second case (figure 2, on the right), TRAF2 and cIAP1/2 are responsible for the stability of NIK (NF-κB Inducing Kinase), that activates NF-κB phosphorylating IKKα [20; 21; 22]. In detail when cells are not stimulated, TRAF2 interacts with TRAF3, which in turn recruits NIK, thus bringing it to the vicinity of cIAP1/2 for K48-linked polyubiquitylation and degradation. This suppresses non-canonical NF-κB activation. Upon receptor stimulation, cIAP1/2 switches substrate specificity from NIK to TRAF2 and TRAF3, allowing NIK to accumulate and activate the non-canonical NF-κB pathway [18]. Recently, it has been shown that RIP1 negatively regulates the non-canonical pathway, confirming that, when RIP1 is active and the receptor stimulated, in the cell a canonical NF-κB is preferred[23]. In the last months the group of professor P. Meier in London discovered that genotoxic stress (*i.e.* induced by etoposide) triggers the formation of a RIP1-Dependent Caspase 8-Activating Platform of 2 MDa, named Ripoptosome (figure 2, centre). In fact, etoposide-mediated depletion of cIAP1, cIAP2, and XIAP causes spontaneous association of the proteins RIP1/FADD/caspase-8. This complex can stimulate caspase-8-mediated apoptosis as well as caspase-independent necrosis.

Importantly, the formation of the complex occurs independently of the involvement of TNF and upstream of mitochondria. The Ripoptosome is inactivated by cIAP1, cIAP2, and XIAP in a Ub-dependent manner, most likely by targeting RIP1 and components of the Ripoptosome for proteasomal degradation. Furthermore, etoposide-mediated loss of IAPs and Ripoptosome formation converts pro-inflammatory cytokines into pro-death signals[24; 25; 26].

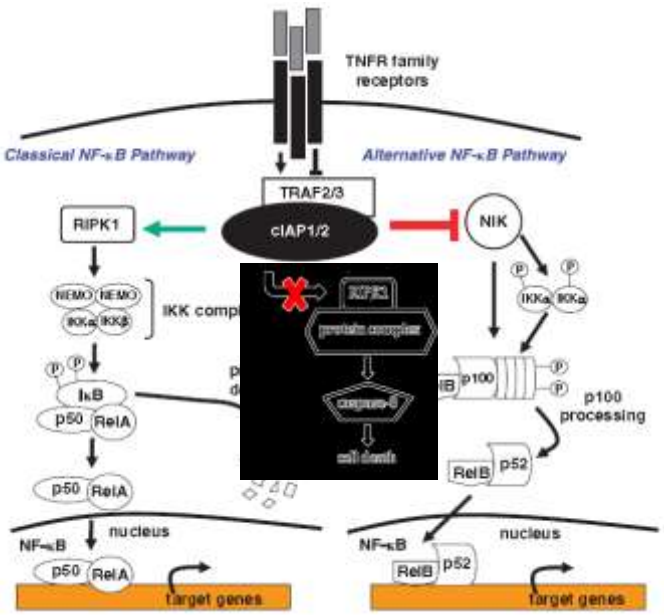

Figure 2. cIAPs positively modulate the classical pathway, or negatively regulate the alternative pathway[18]. **(Left)** In the classical pathway, NF-κB dimers (for example, p50/RelA) are retained in the cytoplasm by interaction with IκB. Upon the binding of TNF-ligand to the TNF-receptor, TRAF proteins are recruited together with the cIAP1/2 complex, and the RIPK1 is K-63 ubiquitylated by the E3 ligase domain of cIAP1/2. The IKK complex is recruited and activated. The activated IKK complex in turn phosphorylates the inhibitor of kB (IkB), leading to its degradation, thereby releasing p50/RelA to translocate into the nucleus for transcriptional activation of targeted genes. **(Right)** cIAP1/2, TRAF2 and TRAF3 represses the alternative NF-kB pathway by promoting the ubiquitination and degradation of NIK, which is required for phosphorylation of p100 in the p100/RelB complex. Phosphorylated p100 is processed into p52, and the p52/RelB dimer translocates into the nucleus for transcriptional activation of targeted genes. **(Centre)** Depletion of IAPs promotes the association of RIPK1 with caspase-8 to form the Ripoptosome, which activates caspase-8-mediated apoptosis.

Smac-DIABLO and the origin of Smac-mimetics

In response to pro-death stimuli the mitochondrial outer membrane permeabilization (MOMP) allows the release of cytocrome c and of one of XIAP endogenous antagonists, Smac-DIABLO (Second Mitochondria-derived Activator of Caspases - Direct IAp Binding protein with LOw pI[27; 28]). Structural and binding studies established that such antagonizing effect is mainly triggered by the Smac-DIABLO N-terminal IBM (IAP Binding Motif), which is composed by four residues (AVPI) and specifically docks into a conserved groove in BIR3 domain of XIAP [29; 30]. This interaction releases caspase-9 that, exposing a conserved IBM on its N-terminus (ATPF), can be competitively recognized and inhibited by the XIAP-BIR3 domain [31; 32] (figure 3).

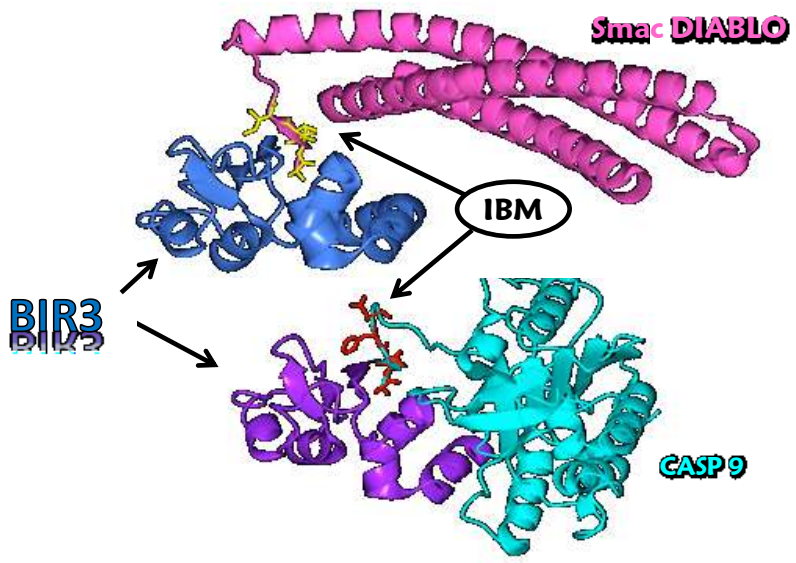

Figure 3. Comparison between the complexes XIAP-BIR3/Smac-DIABLO and XIAP-BIR3/caspase9. The XIAP-BIR3 molecules are represented in light blue and purple, respectively. Smac-DIABLO (magenta) and caspase 9 (cyan) share the Iap Binding Motif (yellow and red for Smac-DIABLO and caspase 9, respectively), that provides the base for Smac-mimetics design.

The molecular mechanism by which Smac-DIABLO recognizes XIAP is not completely understood and X-ray techniques could be very useful to elucidate the structure of this macromolecular complex. For instance, in 2000 the crystal structures of Smac-DIABLO alone and in the presence of XIAP-BIR3 [30; 33] together with biochemical experiments showed that Smac is a dimer and is able to simultaneously bind to two molecules of BIR3. These results suggested an hypothetic model where Smac-DIABLO could recognize both BIR3 and BIR2 of XIAP intramolecularly, thus relieving both effector and initiator caspases activity. However, the estimated affinity of AVPI for the BIR2 domain is quite low compared to the one for BIR3 and maybe this could be the reason why this model has not been confirmed yet. Kulathila et al. [34] obtained the structure of Smac-AVPI in complex with the cIAP1-BIR3 domain and suggested that cIAPs could also bind to Smac-DIABLO in order to prevent its inhibitory activity on XIAP. Anyway, all these data gave birth to a cascade of structure-based drug design studies, where the tetrapeptide AVPI represents the base for the formulation of libraries of peptide mimetic compounds to be developed and screened *in vitro* and *in vivo* within pre-clinical and clinical research, named Smac-mimetics. Although initially designed for targeting XIAP-BIR3, these small molecules have shown to bind also to XIAP-BIR2 and cIAPs-BIR3 with high affinity [35]. Smac-mimetics combine a high specificity with great versatility since they are not cytotoxic and specifically target only BIRs, which in turn are endowed with various roles (as mentioned in the previous paragraph), being implicated in different pathways. Upon binding, Smac-mimetics prevent XIAP inhibition of both initiator and executioner caspases; at the same time, they induce the auto-ubiquitylation and degradation of cIAPs, through a mechanism that is unknown. cIAPs depletion by Smac-mimetics promote the accumulation of NIK and the release of RIP1, which is available to form the

Ripoptosome. The apoptotic signal is then restored and amplified. Anyway, Smac-mimetics are effective only on "SM-sensitive" cancer cell lines, which have been shown to produce autocrine TNF-α upon NF-κB activation[20; 36]. Cells that do not produce TNF-α are "SM-resistant". For this reason the strategy proposed for apoptosis induction is the administration of both Smac-mimetics and TRAIL (Tumor Necrosis Factor-Related Apoptosis-Inducing Ligand), a member of the TNF superfamily of cytokines, which is known to induce apoptosis *in vivo* without causing toxicity to normal cells. In fact, it has been extensively shown that Smac-mimetics treatment enhances TRAIL- or TNFα-mediated cancer cell death[22; 37; 38; 39], since the TNF receptor needs to be stimulated for the Smac-mediated inhibition of cIAPs activity. The roles of IAPs and of IAPs antagonists (Smac-mimetics) in the regulation of apoptosis and NF-κB signaling are summarized in figure 4 [40].

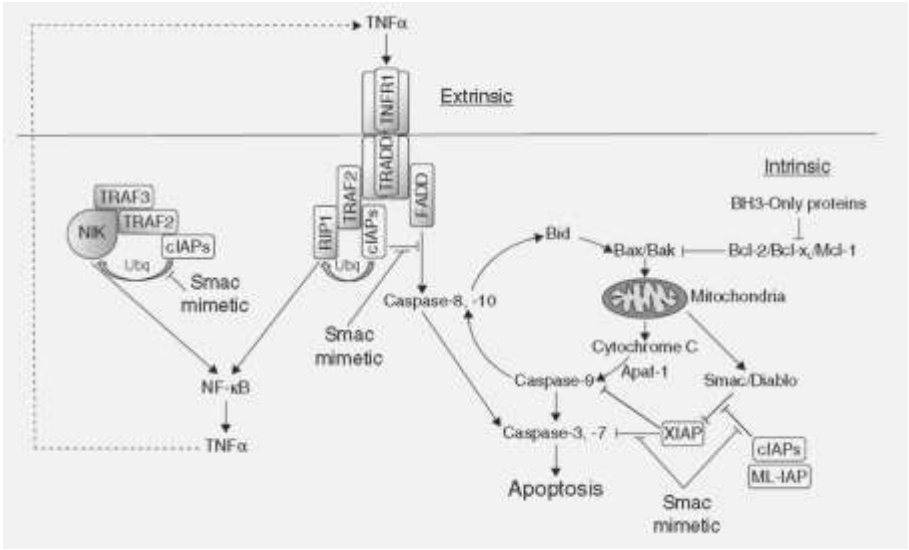

Figure 4. (Left) The extrinsic apoptotic pathway is activated when death receptors, such as TNFR1, are engaged by their respective ligands. This results in recruitment of the adaptor protein FADD and the initiator caspase-8. Auto-processing of caspase-8 results in processing of and activation of the effector caspase-3 and -7. **(Right)** The intrinsic apoptotic pathway is initiated by activation of BH3-only proteins in response to cellular

stresses. Activated BH3-only proteins neutralize the anti-apoptotic Bcl-2 family members, leading to disruption of the mitochondrial membrane potential and release of cytochrome c and Smac/DIABLO into the cytoplasm. Cytochrome c associates with Apaf-1, resulting in activation of caspase-9 and subsequent activation of caspase-3 and -7. IAP proteins represent the last line of defense against inappropriate cell death as they inhibit activated caspase-3, -7 and -9 (XIAP), as well as TNF-α-mediated activation of caspase-8 (cIAPs). IAP proteins can also prevent the endogenous IAP antagonist, Smac/DIABLO, from blocking XIAP-mediated inhibition of caspases. The cIAP proteins also regulate canonical and non-canonical NF-kB signaling via ubiquitination of RIP1 and NIK, respectively. IAP antagonists (Smac mimetics) induce activation of the canonical NF-kB pathway by inducing rapid autoubiquitination and proteasomal degradation of the cIAP proteins. Loss of the cIAP proteins in turn activates the non-canonical NF-kB pathway through stabilization of NIK. NF-kB activation leads to induction of NF-kB target genes, including TNF-α, which can subsequently activate caspase-8 through engagement of TNFR1. The Smac mimetics further enhance apoptotic signals by antagonizing inhibitory interactions between IAP proteins and downstream caspases.

In 2010 the group of Xiaodong Wang in Dallas raised the question of the overcoming resistance to Smac-mimetic-induced apoptosis in some non-responsive cell lines of non-small-cell lung cancer[36]. This study identified a novel mechanism of cIAP2 expression modulation, whereby cIAP2 levels are detectable after a few hours from the treatment with Smac-mimetics. In fact, it has been shown that within cIAP1/2 complex, only cIAP1 is able to auto-ubiquitylate. This means that, upon treatment with Smac-mimetics, cIAP1/2 auto-degrades to completely deplete cIAP1, but basal levels of "cIAP2 left overs" rebound and trigger a positive regulation of cIAP2 expression. cIAP2 is then free to complex again (cIAP2/2) and perform its anti-apoptotic action and, lacking the ability of auto-ubiquitylation, the complex is refractory to subsequent degradation.

How to design a Smac-mimetic

The tetrapeptide AVPI, that is the bases for Smac-mimetics design, is quite conserved among species and since crucial residues are conserved, also essential hydrogen bonds are retained throughout species (figure 5). AVPI binding affinity for XIAP-BIR3 is ~0.5 μM[29].

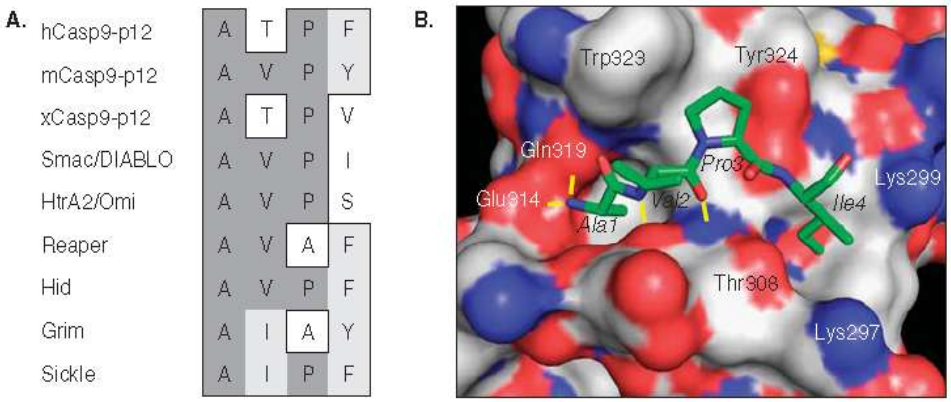

Figure 5. (A) Amino-acid sequence alignment of the four N-terminal residues, constituting the IBM, of the small subunit of active human, murine and Xenopus caspase-9; active mammalian Smac/DIABLO and HtrA2/Omi; and Drosophila Reaper, Hid, Grim and Sickle. Dark and light gray shading indicate identity and similarity, respectively. **(B)** Solvent-accessible surface representation of the peptide-binding site of XIAP–BIR3 in complex with the Smac/DIABLO IBM, AVPI (PDB code 1G73). Conserved hydrogen bonds between the peptide and the protein are indicated in yellow[40].

At the beginning of 2002 Smac-derived peptides have been shown to sensitize a number of different tumor cell lines to apoptosis induced by a variety of pro-apoptotic molecules, both *in vitro* and *in vivo* [41; 42]. Nevertheless, the use of these peptide-based compounds remained limited because they lack proteolytic stability and the cell permeability required to penetrate the cell membrane. This is the reason why in the last years peptidomimetics are preferred by many laboratories and companies. The term peptidomimetic is defined broadly as a peptide-like molecule that has

modifications relative to a native peptide structure that will not occur naturally (such as incorporation of non-natural amino acids, backbone alterations or peptide bond isosteres).

A classic Smac-mimetic contain an N-methyl alanine in the P1 position, which appears to provide adequate protection from proteases while maintaining critical hydrophobic and charge-charge interactions with the IAP-BIR domains. Similarly, most compounds also retain the hydrogen-bond donor and acceptor groups associated with the P2 position of the peptide. This can be achieved by substituting the P2 valine residue with bulkier non-natural amino acids or by introduction of appropriate cyclization in this region of the molecule, both of which can improve potency and/or stability. The most varied region of Smac-mimetics revealed by analysis of the available patents and patent applications is that corresponding with the P3 and P4 positions of the tetrapeptide. In general, the goal of substitutions in this region is to position a hydrophobic moiety for optimal interaction with the P4-binding pocket of the BIR domains. A general picture of the SAR (structure-activity relationship) analysis on Smac-mimetics is reported in figure 6.

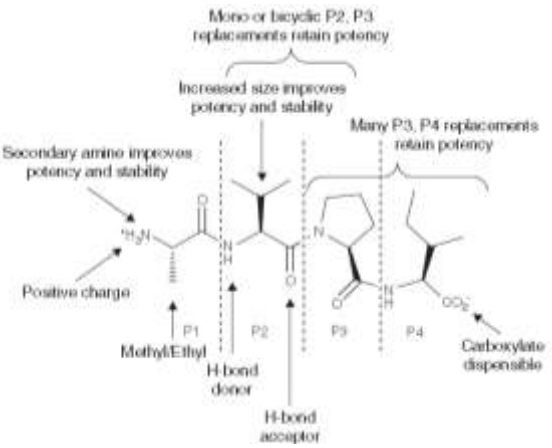

Figure 6. Summary of the SAR trends that in the last years have been reported to optimize Smac-mimetics design[40].

Smac-mimetics can be divided into two big classes, monovalent and divalent ones. The first class was developed to target single BIR domains and was typically designed against XIAP-BIR3[43]. In 2006 our group together with CISI generated a library of 4-substituted azabicyclo alkane [5,3,0] starting from Smac001 (figure 7, panel A), proposed by Sun *et al.* in 2004. As suggested by our crystallographic studies, in 2008 we reported Smac037 from our library (figure 7, panel A) as one of the most potent monovalent compound on XIAP-BIR3 and –BIR23 *in vitro* known to that date, revealing an IC_{50} value of 250 nM when tested on XIAP-BIR3[44]. Unfortunately, Smac037 presented unsatisfactory permeability values upon ADMET tests performed *in vitro*, and therefore, modifications have been supplied to improve bioavailability of the Smac-mimetics from our library (Smac066, in figure 7, panel A).

The second class of Smac-mimetics is represented by divalent compounds able to simultaneously recognize two BIR domains. This recognition can occur intramolecularly, when one divalent compound binds to BIR2 and BIR3 of the same IAP molecule, as mentioned for the model of XIAP and Smac-DIABLO proposed by Chai *et al.*[33], or intermolecularly, when one divalent Smac-mimetic binds to two BIR3 domains belonging to two different IAP molecules, as mentioned by Feltham *et al.* [45] who proposed this kind of binding as involved in the activation of E3 ligase activity of cIAPs and degradation. In both cases, it can be noticed that divalent Smac-mimetics appear as very potent compounds in respect to monovalent compounds. In fact, new trends in literature even suggest that an intramolecular binding is actually preferred in the case of XIAP, releasing both initiator and effector caspases upon treatment with divalent molecules, whereas the intermolecular binding seems favored in the case of cIAP1/2, that act as eterodimers and whose BIR3 domains could be

simultaneously recognized and approached to promote respective RING domains dimerization and stimulation of E3 activity. Anyway, real experimental evidences about these hypotheses are missing and *ad hoc* structural studies to design small molecules capable of distinguishing the two kinds of binding have not been implemented yet. The first divalent Smac-mimetic appeared in literature was compound 3 (figure 7, panel B) by Li *et al.* [46]. Compound 3 was reported as a potent caspase-3 and -9 activator and to test its potency *in vivo* was tested on T98G human glioblastoma cell line, which is resistant to DNA damage-induced apoptosis. When used in combination with TRAIL, 100 nM of Compound 3 cause extensive cell death, and pro-caspase 8 activation was visible at 100 pM. To date one of the most promising compounds reported in literature as active in mice-xenografted breast cancer cells is SM164 by Lu *et al.*[38], showing low nanomolar affinities for XIAP- and cIAPs-BIR3 and -BIR2BIR3 domains. The IC_{50} for this compound in MDA-MB231 breast cancer cells and SK-OV3 ovarian cells is reported to be less than 10 nM. Taking advantage of the experience gathered with monovalent Smac-mimetics[44; 47], our group generated a library of homo- and etero- dimeric Smac-mimetics, composed of two identical or slightly different mimic heads joined by a variety of linkers, in order to explore various rigidity patterns, that would modulate a simultaneous binding, and to test respective metabolic assumption (figure 7, panel B). All the compounds here reported (figure 7) in past years and during this work were subject to crystallization trials with successful results and were chosen from the library according to their IC_{50} values *in vitro* and on some of the cancer cell lines available from collaborators (see The Project Workflow in the next Paragraph). Furthermore, previous to crystallization, their biochemical behavior was analyzed through thermofluorimetric assays,

analytical gel filtration experiments, dynamic light scattering measurements and *in silico* simulations as well.

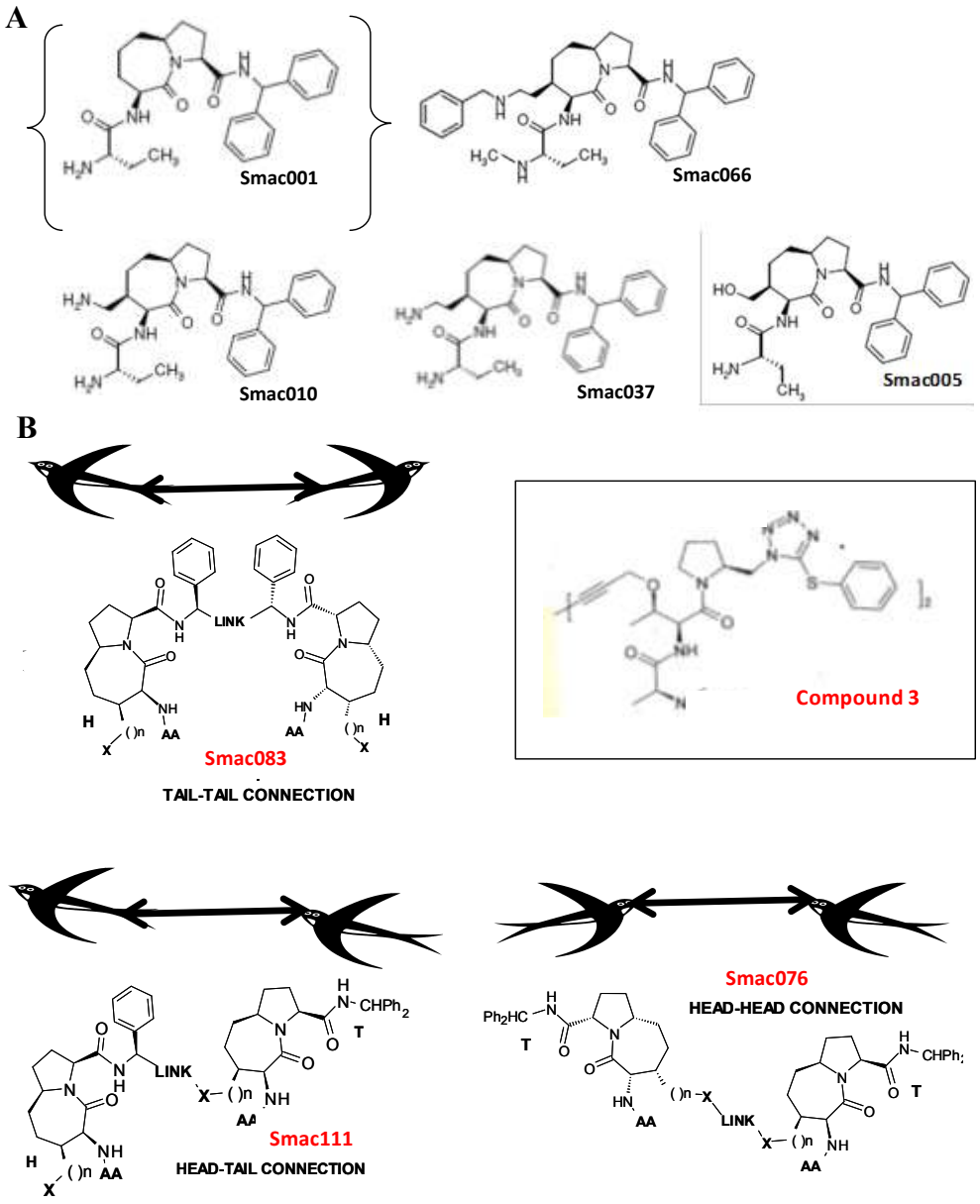

Figure 7. Some of the Smac-mimetics from our library. **(A)** The starting point for the design of monovalent compounds, Smac001, is reported in brackets. Our Smac-mimetics present different substitutions in the fourth position of the seven-carbon ring in the central scaffold. **(B)** Compound 3 was the first divalent compound reported in literature on

Science in 2004, showing potent induction of caspase activation and of apoptosis in human cancer cells upon co-treatment with TRAIL. Our divalent compounds are classified in tail-tail, head-to-tail and head-head according to which part of the mimic head is sacrificed for the design of the linker portion. The chemical nature of the linker and of the "X" substitutions is covered by a patent that is now under revision.

Smac083 (figure 7, panel B) presented remarkable IC_{50} values when tested through fluorescence-based assays on the IAPs constructs produced in our laboratory (BIR3 from XIAP, cIAP1 and cIAP2, and BIR2BIR3 from XIAP). Moreover Smac083 showed very promising data *in vivo*, being able to enhance the MST of mice inoculated with IGROV-1 human ovarian carcinoma cells and to inhibit the cancer growth in xenografted mice. This compound is now the subject of a patent involving all the research groups belonging to the project. Over the past 10 years more than 50 patents and patent applications pertaining to IAP antagonists have been published and a few of them (see table below) have entered or been approved to enter human clinical trials, which will hopefully allow the utility of this potential therapeutic approach to be evaluated in cancer patients[40].

Organization	Compound name	Condition	Clinical stage
Genentech	GDC-0152	Locally advanced or metastatic solid malignancies, or non-Hodgkin's lymphoma without leukaemic phase	Phase I
Novartis Pharmaceuticals	LCL161	Advanced solid tumours	Phase I
TetraLogic Pharmaceuticals	TL32711	Solid tumours and lymphomas	Phase I
Ascenta Therapeutics	AT-406	Advanced solid tumours and lymphomas	Phase I
Human Genome Sciences	HGS1029	Advanced solid tumours and lymphomas	Phase I

Aim of the Project

The project started in 2006 and since then required the collaboration of many groups, connecting chemistry, biochemistry, molecular biology, *in vitro* profiling through cell-free and cell-based assays, structural biology and computational studies. To complete our research framework since 2009 the project gained the chance to test in-house the best compounds on IGROV-1 cells xenografted on mice, thanks to the collaboration of the researcher Paola Perego, PhD from the Istituto Nazionale dei Tumori. All the groups bring the scientific expertise required to undertake this drug design and development project.

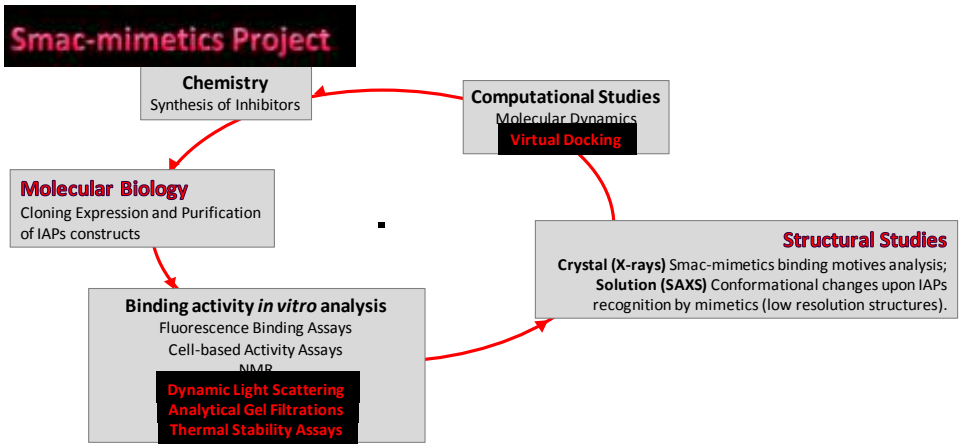

Workflow 1. The Smac-mimetics Project connects different research lines in the field of drug design and discovery. The structural contribute (on the right) is crucial for the project, being in charge of designing and optimizing all the compounds synthesized and of studying macromolecules and protein complexes. Furthermore, our group is responsible for cloning, expressing and purifying all the IAPs constructs of interest, analyzing their biochemical and biophysical behavior and, finally, performing computational studies including Virtual Docking searches on "un-crystallizable" protein/ligand complexes and Virtual Screening of libraries of known compounds available on-line (LOPAC: Library Of Pharmacologically Active Compounds [www.sigmaaldrich.com]) to be tested on our protein constructs.

The main aim of the project is the development of novel Smac-mimetics targeting XIAP-BIR2 and -BIR3 domains, as single molecules or as double-headed inhibitors. The same approach will be extended to XIAP homologues, such as cIAP1 and cIAP2, in order to impair all the functions that IAPs are endowed with and strongly trigger apoptosis *in vitro*, on cancer cell lines, and *in vivo*, on animal models. Since different members of the IAP family cover different roles in the process of apoptosis, structural studies are planned to develop specific IAP-antagonists, in order to analyze distinct apoptotic pathways and elucidate the precise roles fulfilled by Smac-mimetics in the cell. One of the most challenging aims of this project is to answer interesting biological questions that today remain unclear. For example, (1) the recognition of XIAP by Smac-DIABLO or (2) the reason why cIAPs degrade themselves upon binding to Smac-mimetics, but also (3) how could be possible to overcome Smac-mimetics resistance in some cancer cells where cIAP2 is not degraded and exploits its anti-apoptotic function. In order to answer these questions, the full length constructs of the proteins involved in this study (such as Smac-DIABLO, cIAP1 and TRAF2) are required and their structures alone or complexed, even at low resolution, would allow to better understand how they communicate with their partners and by which molecular mechanism they exploit their functions. Furthermore, virtual docking simulations can represent useful tools to optimize Smac-mimetics, to analyze the putative binding mode of developed compounds when crystals are missing and, finally, to find new interesting molecules supporting the current treatments, from the screening of on-line available libraries (*i.e.* LOPAC - www.sigmaaldrich.com) containing compounds already tested in humans. If successful, this strategy would speed the research pipeline up to about ten years.

Main Results

All the BIR constructs considered in this work (XIAP-BIR2BIR3, XIAP-, cIAP1- and cIAP2- BIR3) have been cloned, expressed and purified as described in Cossu *et al.* [47]. Particular procedures have been developed for over-expression of large proteins, such as Smac/DIABLO, cIAP1 and TRAF2, for which clear cloning and purification protocols were absent in literature. The purity level required for crystallization is relatively high and was evaluated by SDS-page as higher than 95%. Monodispersity, measured by DLS (Dynamic Light Scattering), has also to be considered for the determination of sample homogeneity, which is essential for performing good structural experiments and yielding protein crystals.

	R_H (nm)	Polydispersity (%)	Polymerization status and Shape
XIAP-BIR3	2.4±0.1	< 10	Monomeric, globular
XIAP-BIR23	3.0±0.1	< 5	Monomeric, elongated
cIAP1-BIR3	2.5±0.1	< 15	Monomeric, globular
cIAP2-BIR3	2.6±0.1	< 20	Monomeric, globular
XIAP-BIR1	2.6±0.1	<15	Dimeric, globular
cIAP2-BIR1	2.2±0.1	< 25	Monomeric, globular
Smac/Diablo	5.5±0.1	< 15	Tetrameric, very elongated
cIAP1	5.8±0.1	< 20	Monomeric, very elongated
TRAF2	5.5±0.3	< 20	Trimeric, very elongated

Table 1. Summary of DLS measurements on the constructs considered in this work in solution at a concentration of 1 mg/ml. R_H is the hydrodynamic radius expressed in nm, experimentally measured after 20 reads which are performed every 30 seconds. Polydispersity is intended as the presence of multiple species (monomers, dimers, trimers…) in the protein sample and for good quality structural experiments it has to be <20-30%, indicative of homogeneous samples. On the base of the measured radius, the software estimates the molecular weight of the protein in the sample, to be compared with the M_W observed in the SDS-page in order to verify the polymerization status of the protein species in solution. The Mw is calculated assuming that the proteins are globular.

This calculation is quite reliable for the single BIR domains, but in the case of large proteins also the axial ratio has to be considered. Assuming that the protein molecule is a sphere or an ellipsoid, the axial ratio is the ratio between the major and the minor semi-axes and is always included between 1 and 10. For this definition, the table reports proteins with axial ratio similar to 1 as spheric or *globular*, proteins with an axial ratio > that 5 as *very elongated* and *elongated* all the other proteins.

1. Biochemical and structural characterization of Smac-mimetics binding to the IAPs-BIR pockets and applications.

Study of Smac-mimetics binding to IAPs. After testing the purity and monodispersity of the protein samples used in this work by SDS-page and DLS, a biochemical characterization of Smac-mimetics binding to the IAP-BIR domains was addressed through thermal shift assays and analytical size exclusion chromatography. These two techniques have been useful to verify at first the thermal stability gain of the BIRs in the presence of monovalent and divalent compounds and, then, the ability of divalent mimetics to induce a dimerization of the BIR3 domains or a closure of the XIAP-BIR2BIR3 domain, indicative of a simultaneous recognition of both BIR2 and BIR3 by the two mimic heads of the divalent compound.

Thermal shift assay is an experimental technique monitoring florescence variations reported by a protein-bound dye during protein thermal denaturation. The assay is based on the fact that a small molecule by binding to a protein can stabilize its structure and affect the melting temperature (T_M). Table 1.2 reports the stabilization brought by the Smac-mimetics to the BIR constructs as the difference between the T_M of the adducts and the T_M observed for the apo-proteins.

	XIAP-BIR3 (54.8±0.9°C)	XIAP-BIR2BIR3 (46.5 ± 0.7 °C)	cIAP1-BIR3 (58.7 ±0.3 °C)	cIAP2-BIR3 (49.1±0.8 °C)
1	+ 19.8	+ 11.6	+ 27.1	+ 23.6
5	+ 21.4	+ 17.4	+ 28.0	+ 25.2
10	+ 21.0	+ 16.2	+ 24.5	+ 21.8
37	+ 21.2	+ 18.6	+ 25.8	+ 21.9
66	+ 19.0	+ 18.6	+ 24.6	+ 21.1
7	+ 20.0	+ 16.6	+ 25.9	+ 20.8
76	+ 19.8	+ 11.0	+ 22.7	+ 16.8
83	+ 21.2	+ 19.2	+ 28.8	+ 18.5
111	+ 25.4	+ 15.6	+ 25.4	+ 18.6

Table 1.2. Melting temperatures (T_M) increment of the protein constructs (first row, T_M values with standard errors of the proteins alone in brackets) in the presence of monovalent ("1, 5, 10, 37 and 66", first column, second to sixth row of the table) and divalent Smac-mimetics ("7, 76, 83 and 111", first column, seventh to tenth row of the table; "7" corresponds to Compound 3 from Li *et al.*[46]).

Thermal shift assays revealed a global stabilization of the protein constructs in the presence of all the Smac-mimetics here considered, producing an average thermal stability gain of more than 20 °C, especially in the case of cIAP1-BIR3 (Table 1). Although a general accordance between T_M and IC_{50} values obtained in fluorescence polarization assays by our collaborators at Istituto dei Tumori is frequently observed[44; 47; 48], there are not direct methods by which affinity constants can be calculated from thermal stability curves. As a consequence, here T_M values only suggest an increasing stabilization of the adducts produced and are taken as qualitative indication of the affinity ranking for Smac-mimetics towards the BIR constructs. Furthermore, an improved thermal stability has been experimentally correlated with the effective enhanced probability of yielding crystals [49]; in fact, some of the Smac-mimetics that caused the highest T_M, such as Smac005, Smac083 and Smac111, when combined to

the BIR3 domains produced a large number of crystals, increasing the rate of crystallization.

Analytical size exclusion chromatography was used to distinguish the molecular species of the BIR constructs generated in the presence of the divalent Smac-mimetics and of a monovalent compound as a control. Upon binding, compound 3, Smac076, Smac083 and Smac111 at a concentration of 1 mM were able to induce dimerization of XIAP-BIR3 and a closure of XIAP-BIR2BIR3, demonstrating the binding of the two mimic heads to two BIRs simultaneously. In fact, the chromatograms show a peak shift of about –1mL and of +0,4 mL for the complexes XIAP-BIR3/ and XIAP-BIR2BIR3/divalent compounds (Figure 1.1, grey curves), respectively, relative to the apo-proteins (Figure 1.1, black curves).

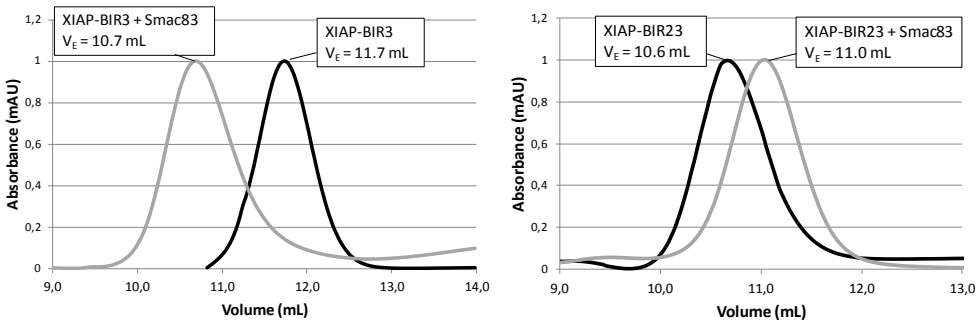

Figure 1.1. Examples of the chromatograms reporting the peaks of the proteins alone and in the presence of 1 mM Smac083. **(Left)** The divalent compound produced a dimerization of the XIAP-BIR3 domain as shown by the peak shift of -1mL towards lower V_E values (corresponding to higher molecular weights; $V_{E\ (XIAP\text{-}BIR3)}$ = 11.8 mL; $V_{E\ (XIAP\text{-}BIR3\ +\ Smac083)}$ = 10.7 mL). **(Right)** Similarly, Smac083 induces a closure of XIAP-BIR2BIR3 as the simultaneous binding of the compound to both BIR2 and BIR3 favors the approaching of the two domains. This is experimentally highlighted by the peak shift towards higher V_E values and, therefore, towards lower apparent molecular weights ($V_{E\ (XIAP\text{-}BIR2BIR3)}$ = 10.7 mL; $V_{E\ (XIAP\text{-}BIR2BIR3\ +\ Smac083)}$ = 11.1 mL). Runs performed with monovalent compounds as control did not produce any peak shift with respect to apo-proteins.

Unexpectedly, higher levels of divalent Smac-mimetics were required to induce cIAP1-BIR3 dimerization which by the way remained partial even after 100-fold SM excess with respect to the protein construct. Partial dimerization could be due to some kind of structural hindrance referred only to the BIR3 of cIAP1, but this hypothesis has to be verified yet.

The crystal structures of the XIAP-BIR3 domain in complex with the monovalent Smac005, Smac010 and Smac037[44; 47] (PDB IDs: 3CM7, 3CLX, 3CM2, 3EYL) but also with the divalent Compound 3[50] (PDB ID: 3G76) allowed us to attempt a structure-based design study through the identification of essential interactions to be preserved and of important modifications to make for improving Smac-mimetics affinity. Thanks to this approach, it was possible to propose Smac037 as potent XIAP-inhibitor, given its complete interactions network established with the XIAP-BIR3 pocket relative to Smac005 and 010, which was subsequently confirmed by X-ray structure[47]. Virtual docking simulations on cIAP1-BIR3 suggested that all the monovalent Smac-mimetics here reported could also bind to the XIAP-BIR3 homologues, although the two IBM-specific pockets present some aminoacidic substitutions. This hypothesis was confirmed by the first structure of cIAP1-BIR3 in complex with a Smac-mimetic (Smac037) reported in literature and solved by our group[48].

Applications: specific Smac-mimetics. As Smac-mimetics inhibit cIAPs and XIAP differently, a structure-based design of cIAPs- or XIAP-specific inhibitors was attempted through the study of Smac-mimetics binding modes observed in our crystals, with the final aim of investigating the different mechanisms in which IAPs play crucial roles. In fact, selectively blocking whether the intrinsic or the extrinsic pathway by administering

XIAP- or cIAPs-specific inhibitors respectively, it could be possible to deeper understand IAPs roles and, generally, to better characterize downstream processes able to trigger apoptosis. In order to design XIAP- or cIAPs-specific Smac-mimetics is essential to find any difference in the two homologue BIR3 active pockets and, eventually, in the neighboring regions. Once designed, the small-molecule has to be tested for its affinity to one or the homologue domain and, finally classified as XIAP- or cIAPs-specific, according to the IC_{50} values obtained. We assumed that if the affinity for one domain is at least 2 orders of magnitude minor than the affinity for the homologue domain, the molecule can be classified as specific. Taking a look to the BIR3 active pockets a few, but crucial, features can be considered to design discriminating compounds. Figure 1.2 reports the alignment of the BIR3 active pockets in XIAP, cIAP1 and cIAP2, highlighting the differences between the BIR3 pockets and the portions of Smac-mimetics to be modified to produce specific compounds.

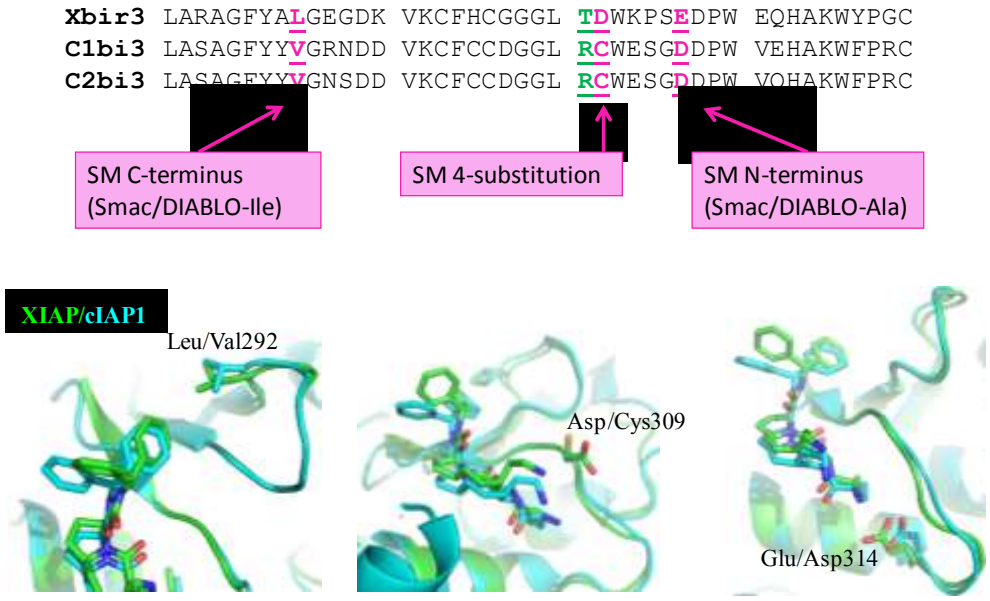

Figure 1.2. (Top view) Alignment of homologous BIR3 active pockets. The substituted residues which have been considered for the design of specific Smac-mimetics (SM) are

shown in magenta (XIAP-Leu292/cIAPs-Val292; XIAP-Asp309/cIAPs-Cys309; XIAP-Glu314/cIAPs-Asp314). XIAP-Thr308 substitution with cIAPs-Arg308 is reported in green, since SM interaction with these residues occurs only through IAPs backbone atoms. The magenta blocks point out which are the SM portions (and corresponding Smac/DIABLO aminoacids) that usually interact with the substituted residues. **(Bottom view) Superposition of XIAP-BIR3 (green) and cIAP1-BIR3 (cyan) structures in complex with Smac037.** Each panel highlights one of the IAPs-BIR3 aminoacidic substitutions considered for the design of specific SM and the portion of Smac037 that interacts with such residues.

The grooves on cIAP1-BIR3 that interact with SM C- and N-termini are slightly wider than the grooves observed in XIAP-BIR3, eventually allowing the positioning of groups characterized by a bigger steric hindrance. For this reason, the addition of methyl or even larger groups on the SM C-terminal phenyl was proposed, to enhance cIAP1-specificity. Furthermore, the SM N-terminal methylation, that has been demonstrated to improve membrane permeability, was also supplied, although it does not seem to impair the affinity for XIAP. SM specificity for cIAP1 can be also reached by modifying the 4-substitution on the SM central ring to get an interaction with cIAPs-Cys309, which is non-conservatively substituted by Asp309 in XIAP-BIR3. The thiol group of Cys309 is nucleophile and reactive. For this reason, several modifications can be adopted on Smac-mimetics, such as the introduction of double bonds to produce Michael adducts. The final result is the formation of covalent bonds, which are incompatible in organisms as too reactive, but could be useful during *in vitro* experiments. It can be noticed that, due to the BIR3 pockets characteristics, cIAPs-specific SM are easier to design and, therefore, have now the priority on XIAP-specific compounds. Prior to crystallization, all the specific Smac-mimetics have been tested in fluorescence polarization assays to determine their IC_{50} values. Generally, a decrease of two orders of magnitude in SM affinity for XIAP-BIR3 with respect to cIAPs-BIR3 is

observed. For example, one of the cIAPs-specific compounds carrying a bulky group on the SM C-terminal phenyl shows a IC_{50} value of 80 nM towards cIAPs-BIR3 and 8 µM towards XIAP-BIR3. Thermofluorimetric assays agree with fluorescence polarization experiments showing that cIAPs-specific compounds bring an average stabilization of 30 °C on cIAP1-BIR3 versus a stabilization of 20 °C on XIAP-BIR3. Crystallization trials of the BIR3 domains in complex with cIAPs- and XIAP-specific compounds have already been implemented, in order to understand at atomic resolution the binding modes of these compounds to both XIAP- and cIAPs-BIR3. Unfortunately, the crystals tested suffered cryogenic conditions or displayed an unsatisfactory diffraction pattern. Optimization of crystallization and cryogenic conditions are now in progress to improve the diffraction pattern.

Applications: improving bioavailability. Despite its potency *in vitro*, Smac037 did not show a satisfactory ADMET profile, since the presence of charged groups, such as the amine group on the 4-substitution of the central ring or the amine corresponding to the Alanine N-terminus from Smac AVPI (Figure 7), affected the ADMET parameters concerning membranes permeability. To facilitate Smac037 crossing through cellular membranes and favor its metabolic assumption, Smac066 was chosen from our library, masking the amines with a phenyl and a methyl group, respectively (Figure 7). The structure of cIAP1-BIR3 in the presence of Smac066 [48] showed that the addition of this bulky phenyl did not impair Smac066 binding mode compared to Smac037, as also confirmed by thermal stability assays and fluorescence polarization experiments. Furthermore, Smac066 displayed greater *in vitro* EC_{50} values (low

micromolar) measured on some cancer cell lines, such as MDA-MB-231, HL60 and PC-3 (unpublished data), suggesting a greater bioavailability.

Applications: planning the design of divalent compounds. When compared to the structure of Smac037 in complex with cIAP1-BIR3, Smac066 presents higher average B values, due to the significant mobility of Smac066 elongated 4-substituent (average B factor of 90 over the four chains) and of the free phenyl from the diphenyl group (average B factor of 100 over the four chains). Such mobile parts can be detected in almost all our structures, as for the structure of XIAP-BIR3/Smac005, which reports high B-factor scores for Smac005 free phenyl and the 4-substitution (Figure 1.3, panel A). As a consequence, such portions of the Smac-mimetics may provide the bases for drug optimization: in particular, since it has been shown that bivalent mimetic molecules could be very effective on tumors alone or in synergy with TRAIL [38], mobile non-interactive portions could be elongated for the design of divalent compounds, that could simultaneously target different intra-molecular BIR domains. For example, the addition of Smac066 4-substituent provide quite general hints for the study of potential bivalent compounds; for this purpose, a non-interactive linker between the two Smac-mimic heads would be preferable, in order to favor the Smac-mimetic/IBM groove interactions only and avoid secondary binding motives, that would produce an impairment of the usual IAPs/Smac-mimetics recognition.

Figure 1.3. (A) Four molecules of Smac005 from the superposition of all the complexes XIAP-BIR3/Smac005 present in the asymmetric unit (PDB id 3CM7). B-factors are indicative of the atoms mobility (B factor values reported in the boxes suggest relatively high mobility levels). **(B)** The addiction of Smac066 (green) 4-substitution and N-methylation do not impair Smac037 (magenta) binding mode to cIAP1-BIR3. **(C)** Smac066 free phenyl and 4-substitution are free in the solvent and could be useful to obtain divalent SM (*i.e.* Smac066 4-substitution presents an average B factor value of 80 indicating high mobility).

The crystal structure of cIAP1-BIR3/Smac066[48] shows that Smac066 free phenyl and 4-substitution seem to meet this requirement, since they are free in the solvent and enough exposed to reach another Smac-mimetic molecule on condition that a few carbons segment would be added (Figure 1.3, panels B and C).

Other Applications. Smac-mimetics mobile parts are also useful for the design of derivatives that can be biotinylated, fused to fluorescent molecules or to nanoparticles to develop new *in vitro* studies and novel strategies for drug delivery.

Structural characterization of the binding mode of divalent compounds. The structural study of divalent compounds binding modes to the BIR domains has been addressed through X-ray crystallography as high resolution technique and through SAXS (Small Angle X-ray Scattering) for the determination of low resolution structures of proteins in solution. The combination of these two techniques allowed a detailed analysis of the binding of double-headed compounds to the active BIR3 pockets, similarly to monovalent SM, and of the scattering pattern shown by XIAP-BIR23 alone or in the presence of the divalent compounds. Such structural characterization was at first performed for Compound 3[50], and afterwards for some divalent Smac-mimetics from our library, which revealed promising IC_{50} values *in vitro* (submitted article). Usually, the structures of XIAP- or cIAPs-BIR3 in complex with divalent compounds have been obtained after a lot of crystallization trials and diffraction experiments, since crystals did not show a single diffraction pattern and appear intrinsically disordered. Consequently, also the analysis of the collected data including the identification of the exact spatial group took several days. Although in the case of Compound 3 a dimer of XIAP-BIR3 in the crystal was not observed, Smac083 from our library was compatible with the dimerization of both cIAP1- and XIAP1-BIR3 domains (Figure 1.4). In the first case, in accordance to analytical gel filtration experiments, a crystallographic dimer of cIAP1-BIR3 was obtained, as the relative positioning of cIAP1-BIR3 molecules in the asymmetric unit recurs in the crystal structures of cIAP1-BIR3 in the presence of monovalent SM. In conclusion, cIAP1-BIR3 dimer in complex with Smac083 was due to crystal packing, which probably drove monomer/dimer equilibrium observed in analytical gel filtrations towards the dimer formation. On the other hand, the relative positioning of XIAP-BIR3 molecules in the crystal

suggests that the protein arranges in dimers only driven by the presence of Smac083.

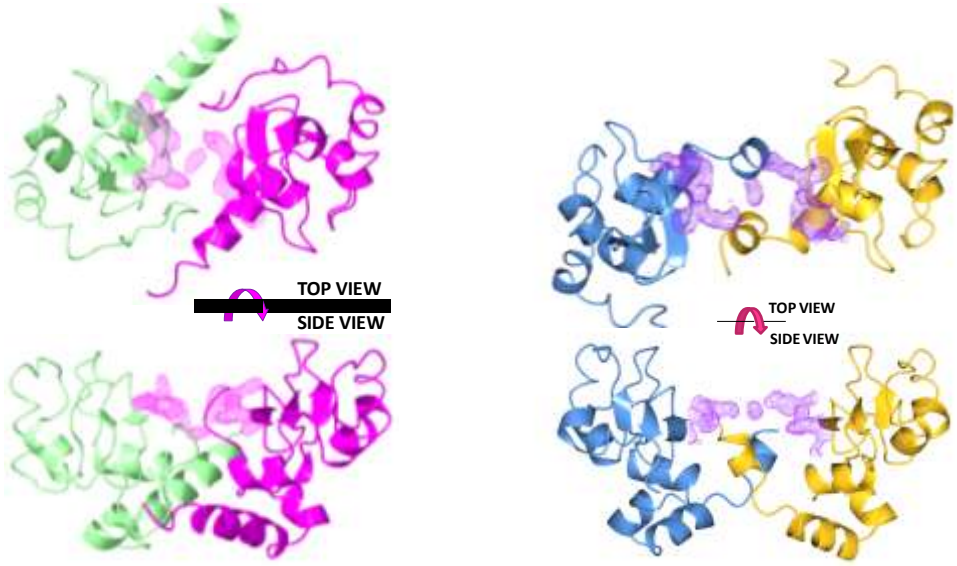

Figure 1.4. Crystal structures of XIAP- and cIAP1-BIR3 in complex with Smac083. **(Left)** XIAP-BIR3/Smac083 complex crystallized in the $P2_12_12_1$ group, showing 4 molecules per asymmetric unit. Two molecules of XIAP-BIR3 (light green and magenta) are bound through one Smac083 molecule (pink density) **(Right)** cIAP1-BIR3/Smac083 structure crystallized in the C2 group with 4 molecules in the asymmetric unit. In contrast to the first complex on the left, the dimer of cIAP1-BIR3 is due to crystal packing as it can be easily compared to the structure of cIAP1-BIR3/Smac037 or 066 which crystallized in the same form. By the way, the presence of one copy of Smac083 (purple density) was compatible with cIAP1-BIR3 dimer (yellow and light blue), with the two Smac083 heads docked into cIAP1-BIR3 active pockets.

Since crystals of XIAP-BIR23 alone or in the presence of divalent compounds were not obtained, samples of the protein alone and in the presence of Compound 3 or Smac083 were taken to the SOLEIL Synchrotron in Paris for SAXS experiments. SAXS is a structural technique used to investigate the shape of both ligand-bound and uncomplexed proteins in solution. The ability to study molecules in solution not only obviates the necessity for crystallization, but also allows to examine the molecule under conditions that leave greater structural

flexibility. This technique is based on the elastic scattering of X-rays interacting with protein samples. The interference of the scattered waves can be related to the spatial distribution of the atoms in the sample. Data are collected as intensities (I) recorded over a range of angles (Θ) and for mathematical convenience, are converted to an intensity function, *I(q)*, related to the scattering vector amplitude, *q*, such that

$$q = 4\pi(\sin \Theta)/\lambda$$

where λ is the wavelength of the X-ray radiation. For monodisperse systems, where particles are randomly distributed with uncorrelated positions and orientations, I(q) is a continuous isotropic function resulting from the sum of the scattering amplitudes of atoms within a finite volume element divided by its volume. I(q) is, therefore, proportional to the scattering from a single particle averaged over all orientations. I(q) can be related to the molecular mass and radius of gyration (R_g) of the molecule by the Guinier equation, which is graphically represented by the Guinier plot (ln[I(q)] versus q^2). For monodisperse systems, the plot is linear and the molecular mass and R_g are provided by the I(0) intercept and the slope of the line, respectively[51].

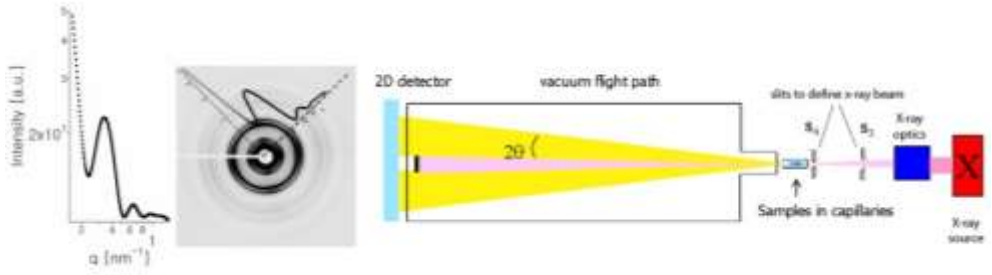

Figure 1.5. Schematic representation of a SAXS experiment. Our experiment was coupled with size exclusion chromatography, to avoid aggregates running through the capillary and favor sample homogeneity. The scattered waves are recorded on the detector and represented in one-dimension plots (on the left). Runs at several concentrations can be integrated to generate one profile for each protein.

By means of Fourier transform, I(q) can be converted into the real space pair distance function, P(r). P(r) represents the frequency of vector lengths connecting small volume elements within the scattering particle, weighted by their scattering densities. The largest of these vectors, corresponding to the maximum dimension of the particle (D_{max}), will have the smallest frequency.

As observed in gel filtration experiments, XIAP-BIR23 undergoes a structural closure upon binding to the divalent Smac-mimetics. In detail, Compound 3 was studied together with the construct of XIAP-BIR23 that includes the N-terminal portion named *linker*, identified with aminoacids 124 – 140. Figure 1.6 reports the shape of linkerBIR2BIR3 alone and after addition of Compound 3 (on the left) and a colored model of linkerBIR2-BIR3 complexed with the divalent Smac-mimetic fitted in the low resolution SAXS structure[50]. The SAXS structures are obtained by two-dimension data using *ad hoc* graphical softwares.

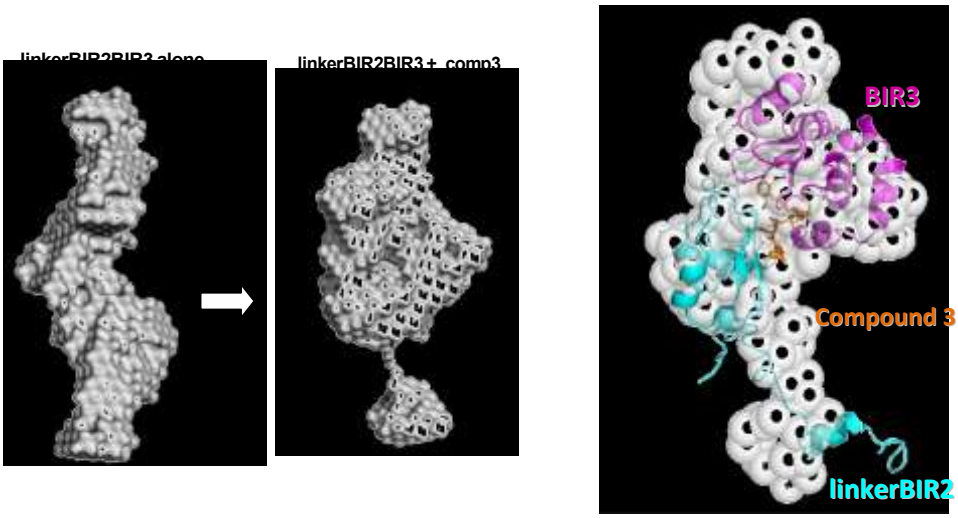

Figure 1.6. SAXS experiments of linkerBIR2BIR3 alone and in complex with Compound3. **(Left, in grey)** The protein construct linkerBIR2BIR3 shows a quite elongated shape in solution and the addiction of Compound 3 to a final concentration of 1 mM triggers the closure of the protein, indicating a simultaneous binding of the SM to BIR2 and BIR3 of XIAP. **(Right)** The SAXS structure of linkerBIR2BIR3 in complex

with Compound3 is shown in white balloons. A model including linkerBIR2 (cyan), BIR3 (magenta) and Compound3 (orange) was fitted by Dr. Mario Milani from the lab.

Analogously, the presence of Smac083 induces a shift in the gyration radius from 25.0 ± 0.2 Å of the apo-protein XIAP-BIR23 to 20.7 ± 0.2 Å of the complex, as showed by the Guinier plot (Figure 1.7).

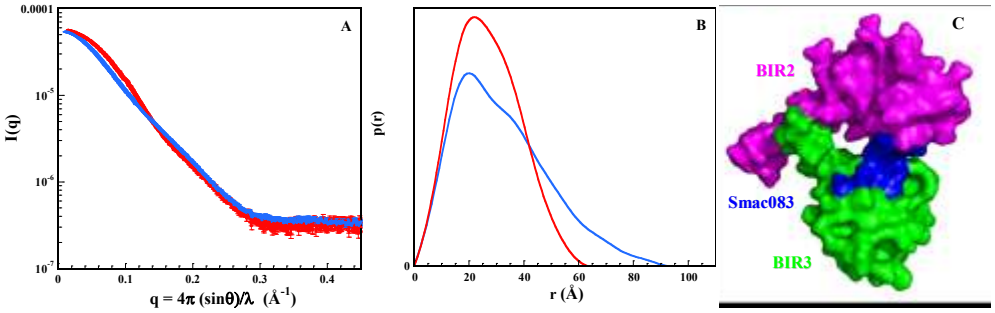

Figure 1.7. Results of SAXS experiments on XIAP-BIR23 alone and in the presence of Smac083. **(A, B)** Experimental curves of XIAP-BIR23 (red) and of XIAP-BIR23/Smac083 (blue) showing the Guinier plot (panel A) and the distances distribution P(r) (panel B). Panel C reports the model of XIAP-BIR23/Smac083 that best fitted the experimental data.

2. Study of XIAP recognition by Smac/DIABLO.

The molecular mechanism by which Smac/DIABLO recognizes and inhibits XIAP remains unknown and has been studied through analytical size exclusion chromatography and SAXS. The molar ratio XIAP ÷ Smac/DIABLO reported in literature is 1 ÷ 1.6, which was verified in this work during analytical GF runs as the ratio where Smac/DIABLO saturated XIAP-BIR23. The elution volume of Smac/DIABLO corresponds to its tetrameric form (as already observed in DLS measurements reported in Table 1), whereas XIAP-lkBIR23 elutes as a monomer. The peak of XIAP-lkBIR23 + Smac/DIABLO is close to the dead volume of the column (~ 8,0 mL) and, by the way, the shift with respect to Smac/DIABLO peak indicates the formation of a macromolecular complex (Figure 2.1).

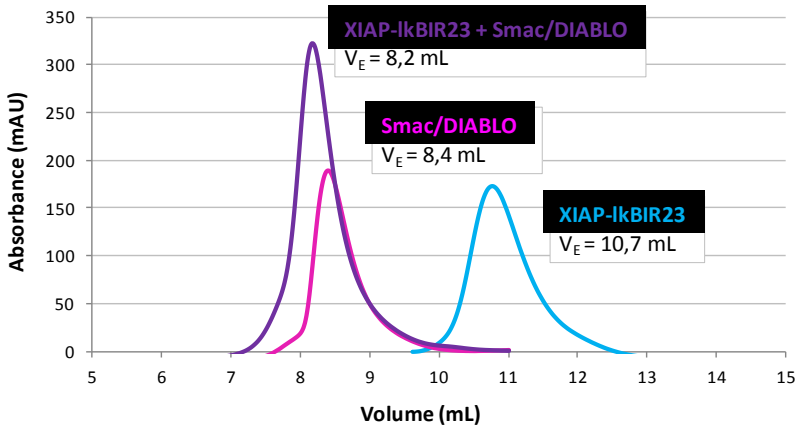

Figure 2.1 Analytical Size Exclusion Chromatography on XIAP-BIR23 (cyan), Smac/DIABLO (magenta) and the complex (purple, molar ratio 1 ÷ 1.6). All the runs were performed on Superdex 75 10/300 GL (GE Healthcare) at constant flow rate of 0.5 mL/min injecting equimolar quantities of all the protein constructs.

Similar chromatograms were obtained at SOLEIL Synchrotron in Paris using Superdex 200 10/300 GL (GE healthcare) where the eluted peaks were subject to X-ray radiation during SAXS experiments. The coupling of size exclusion chromatography to SAXS successfully avoided aggregation of the irradiated samples, which were freezed for transportation. The SAXS results obtained for XIAP-BIR23 are reported in Figure 1.7 (red curves). SAXS data on Smac/DIABLO and on the complex are now under treatment by Dr. Mario Milani from the lab and by Patrice Vachette at the University of Paris-Sud.

In this work the study of Smac/DIABLO oligomeric assembly and of its recognition by XIAP-BIR23 was also addressed through X-ray crystallography and SLS (Static Light Scattering) measurements. In particular, in literature [33] Smac/DIABLO is always reported as a dimer, and, because of its dimeric nature, as able to bind one XIAP molecule. Since it has been extensively shown that Smac/DIABLO is not able to bind to the XIAP-BIR1 domain, the construct XIAP-BIR2 and -3 was considered for the analysis of XIAP-Smac/DIABLO complex. Concerning Smac/DIABLO assembly, different crystal forms of this protein contained quite similar Smac/DIABLO primary dimers (as the one observed in literature), which in turn assemble through secondary dimerization patterns producing a tetramer (Figure 2.2). The formation of a tetrameric assembly in solution is accordingly supported in this work by different techniques, such as SAXS, DLS and SLS experiments mentioned above. In detail, the different primary dimers observed, leading to different types of assemblies, evidence that Smac/DIABLO may undergo some sort of "slippage", thus promoting flexibility and partners binding. In fact, Smac/DIABLO capability of arranging in multiple assemblies might likely be optimized during evolution, to assist and enhance the binding with its

various natural partners, such as XIAP or cIAPs. Futhermore, Smac/DIABLO structure is typical of helical bundles, where the high content of α-helices is often reported to mediate protein-protein interactions (PPIs).

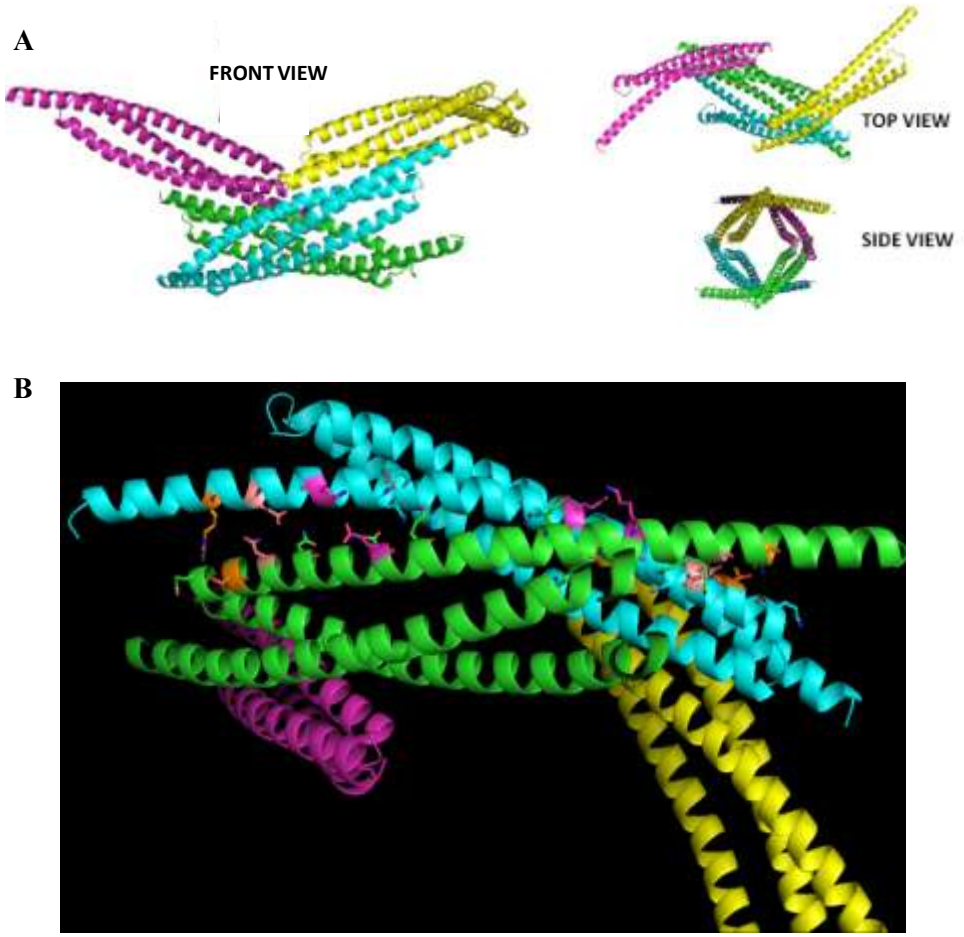

Figure 2.2 (A) Smac/DIABLO assembly in one of the crystal structures obtained by Eloise Mastrangelo from the lab. Primary dimers are the couples magenta/green and cyan/yellow. **(B)** All the interactions stabilizing the secondary dimerization are shown in sticks colored by atoms (red oxygens, blue nitrogens and multicolor carbons). Labels are missing for symmetric interacting residues.

Static light scattering (SLS) is a technique that measures the intensity of the scattered light to obtain the average molecular weight (MW) of a macromolecule, like a polymer or a protein. Measurement of the scattering intensity at many angles allows the calculation of the root mean square radius, also called the radius of gyration (R_g) of the macromolecules in the sample, useful for comparisons with the SAXS results. As in SAXS experiments, SLS was coupled to a Superdex 200 10/300 GL column, in order to examine a pure and monodisperse sample and obtain high quality data. Runs were performed at different concentrations after ultracentrifugation of the samples to exclude protein aggregates.

	V_E (mL)	Molecular Weight (kDa)	Calculated radius (nm)
Smac/DIABLO	12.7	81.4	4.9 ± 0.1
XIAP-BIR23	15.8	30.1	2.9
Complex	12.3	130	9.4

Table 2.1 Summary of SLS measurements on Smac/DIABLO, XIAP-BIR23 (without the N-terminal *linker* portion) and on the complex. Final concentrations were 3.8 mg/ml and 2.5 mg/ml for Smac/DIABLO (the radius was calculated as the average of two runs), 6 mg/ml for XIAP-BIR23 and, finally, 2mg/ml and 1.3mg/ml for Smac-DIABLO and XIAP-BIR23 in the complex, respectively.

SLS measurements confirmed the presence of a Smac-DIABLO tetramer and of a complex containing such tetramer bound to two molecules of XIAP-BIR23. These data, together with crystal structures and SAXS experiments are the subject of a manuscript which is now being written in collaboration with Eloise Mastrangelo and Mario Milani from the lab and Patrice Vachette from the University of Paris-Sud.

3. Design of TRAF2- or TAB1-mimetics to find novel therapies supporting Smac-mimetics.

The IAPs-BIR1 domains were investigated for their anti-apoptotic activity only a few years ago. In detail, XIAP-BIR1 is required for TAB1-dependent TAK1 activation to trigger NF-κB survival pathway, whereas cIAP2-BIR1 are involved in the recognition of TRAFs (Figure 3.1, panel A), which are essential for cIAP1/2 recruiting to the TNF-RSC and their E3 ligase activity. As previously mentioned, Smac-mimetics induce autodegradation of cIAPs through auto-ubiquitylation, but in some cases even Smac-mimetics are not enough for apoptotic induction [36]. In particular, high levels of cIAP2, which is in charge of cIAP1/2 recruiting to TNF-RSC, are detectable even after treatment with SM compounds. The presence of cIAP2 overcomes cIAP1 absence, thus promoting cancer cells resistance to Smac-mimetics. Since cIAPs binding to TRAFs is essential for anti-apoptotic activity, the BIR1 domain of cIAP2 was set as rigid molecule during virtual docking searches. A library containing more than 1200 compounds (LOPAC), which are already pharmacologically characterized, was screened to find a hit able to bind to the surface of cIAP2-BIR1 recognized by TRAF2 [19]. This approach allowed the identification of NF023, an antagonist of P2X receptors known to modulate vasoconstriction, as able to impair cIAP2-BIR1/TRAF2 assembling with estimated low micromolar inhibition constant (Figure 3.1, panel B). NF023 was purchased from SIGMA together with Suramin, the parental NF023 analogue, to be used as control. Furthermore, a *de novo* design of TRAF2-mimetics was started by Dr. Mario Milani from the lab, mimicking the residues of TRAF2 involved in cIAP2-BIR1 binding (Figure 3.1, panel C). Inhibition constants were estimated during virtual docking simulations as low nanomolar in the best cases. Through this

approach a few peptide-mimetics were designed and then synthesized by EZBiolab (http://www.ezbiolab.com).

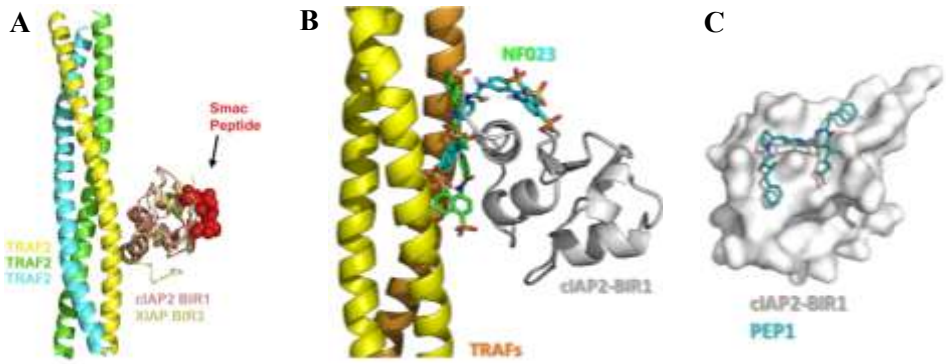

Figure 3.1. Strategy for TRAF2-mimetics design. (A) cIAP2-BIR1 (pink) binding with TRAF2 (yellow/green/cyan) involves interactions between α-helices. A superimposition of cIAP2-BIR1 on XIAP-BIR3 reveals that putative Smac-mimetic binding occurs far away from the surface engaged in the interaction with TRAF2. **(B)** Two conformations of NF023 (cyan and green, average free energy of binding -8.5 kcal/mol) are modeled according to the results of virtual docking. The positioning of NF023 impairs in both cases cIAP2-BIR1/TRAF2 binding. **(C)** cIAP2-BIR1 surface in complex with PEP1, one of the TRAF2-mimetics *de novo* designed by Dr. Mario Milani from the lab.

A structural superimposition of the two homologous BIR1 from the complex cIAP2-BIR1/TRAFs (PDB id: 3M0D) and XIAP-BIR1/TAB1 (PDB id: 2POP) reveals that the surface of cIAP2-BIR1 involved in TRAF2 recognition corresponds to the portion on XIAP-BIR1 engaged in the interaction with TAB1 (Figure 3.2, A). As in the case of Smac/DIABLO, the surfaces implicated in the protein-protein interactions are characterized by high α–helical content. A virtual docking on XIAP-BIR1 was performed to verify NF023 *in silico* ability to impair also XIAP-BIR1/TAB1 binding. In this case NF023 showed estimated free energies of binding much lower with respect to the previous run on cIAP2-BIR1.

Surprisingly, NF023 was shown not only to block XIAP-BIR1 recognition by TAB1, but also XIAP-BIR1 dimerization which is reported to be essential for TAB1 activation (Figure 3.2, panel B).

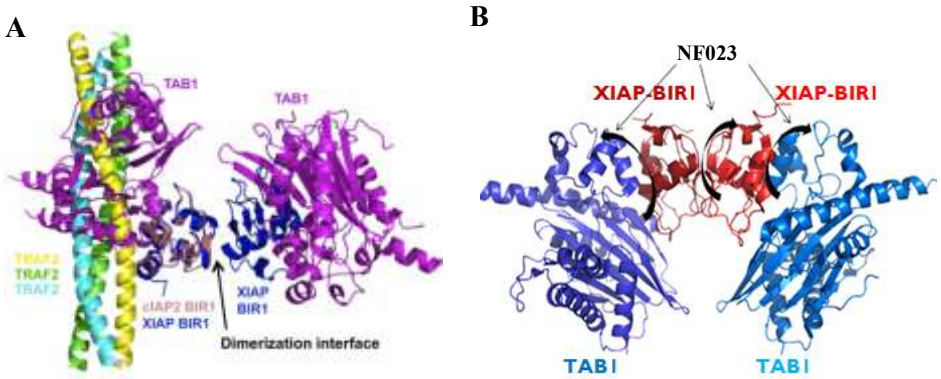

Figure 3.2 Strategy for TAB1-mimetics design. (A) Superimposition of the complexes cIAP2-BIR1/TRAF2 and XIAP-BIR1/TAB1. **(B)** Virtual docking results on XIAP-BIR1 (red) set as rigid. Two conformations of NF023 (black arrows) displayed average values of free energy of binding of -9 kcal/mol (estimated k_i= 300 nM). Both predicted conformations could effectively block for TAB1 inactivation.

The BIR1 domains of interest were cloned, expressed, purified and characterized by SDS-PAGE, DLS (see first table in Main Results) and thermal stability assays. All the Smac-mimetics tested did not bring significant melting temperature variations with respect to the apo-proteins, whereas NF023 or Suramin heavily destabilized the protein constructs.

	cIAP2-BIR1 (T_M=61.5±0.7°C)	XIAP-BIR1 (T_M=59.3 ±0.4°C)
1	-1.5°C	-2.1°C
5	-0.6°C	-0.4°C
37	-1.7°C	-0.8°C
66	+0.5°C	-2.1°C
83	-3.4°C	-2.5°C
76	-4.2°C	-2.9°C
111	-2.0°C	-2.1°C

	cIAP2-BIR1	XIAP-BIR1
NF023	-27.1°C	-10.5°C
Sur	-25.6°C	-14.6°C
PEP1	-8.7°C	/
PEP2	-6.5°C	/

Table 3.1 ΔT_M calculated between the T_M values of the proteins in the presence of Smac-mimetics (1-111) and of novel putative inhibitors (NF023, Suramin, PEP1, PEP2) and the T_M values of the proteins alone. Since they were designed on cIAP2-BIR1, PEP1 and PEP2 were not tested on XIAP.

Despite discouraging T_M values, crystallization trials of cIAP2-BIR1 and XIAP-BIR1 alone and in the presence of all the novel inhibitors and of Smac037 from our library were set up. Quasi crystals of cIAP2-BIR1 were obtained, leading to powder diffraction and very fragile crystals of cIAP2-BIR1 with PEP2 dissolved when sealed in cryoprotectant solution. Rhombic crystals of XIAP-BIR1 alone and in the presence of Smac037 and NF023 were obtained and optimized to produce good quality crystals. Unfortunately, the crystals of XIAP-BIR1/Smac037 did not show a good quality diffraction pattern and are now under optimization.

The crystal structure of XIAP-BIR1 is identical to the one reported in literature (PDB id: 2QRA) displaying 4 molecules per asymmetric unit arranged in two dimers (Figure 3.3). The dimers are stabilized mainly by electrostatic interactions between the two parallel β1 strands and between crucial residues (Figure 3.3, zoom) belonging to α1, α1- β1 loop and β2 strand from the two different BIR1 molecules.

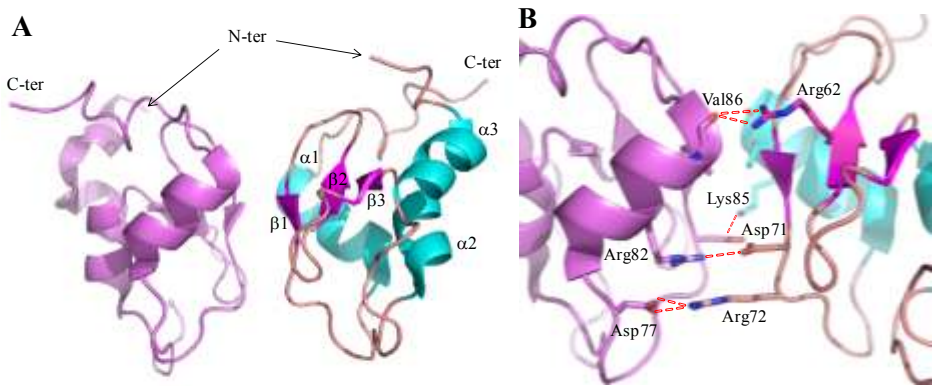

Figure 3.3 Crystal structure of XIAP-BIR1. (A) XIAP-BIR1 dimer observed in the crystal stabilized by the two central β1 strands that face parallely. **(B)** Zoom of the dimer interface area with interacting residues highlighted in sticks.

XIAP-BIR1/NF023 crystallized in the same form of the apo-protein crystal. The crystal of XIAP-BIR1/NF023 diffracted at 2.1 Å of resolution and the structure was refined to reach R_{factor}/R_{free} values of 20.3/26.0. During refinement residual electron density was modeled as NF023, but its positioning did not confirm the virtual docking simulations. In fact, the inhibitor was predicted to disrupt XIAP-BIR1 dimer (Figure 3.4), but actually the protein maintained the dimeric arrangement despite the presence of NF023. The only perturbation of XIAP-BIR1 dimer was shown to be a slight shift of one BIR molecule with respect to the partner, revealed by the superimposition of XIAP-BIR1/NF023 structure to the one of the apo-protein (Figure 3.4).

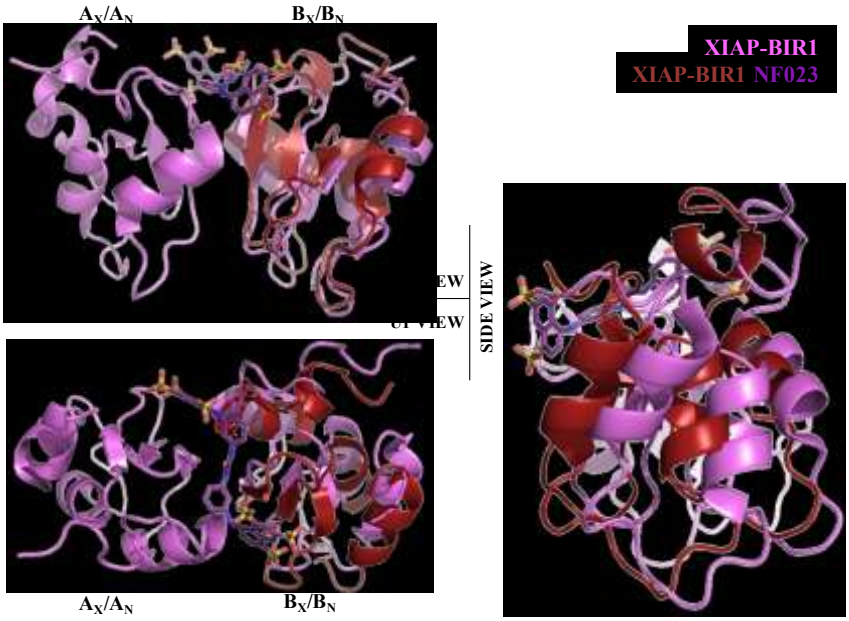

Figure 3.4 Superimposition of chain A_X from XIAP-BIR1 and chain A_N from XIAP-BIR/NF023 structure. The dimer of XIAP-BIR1 composed of chains A_X and B_X is reported in pink, whereas the shifted chain B_N is reported in red. The shift of chain B_N with respect to the position of B_X is about 3 Å.

NF023 binding to XIAP-BIR1 is stabilized by few interactions. In details, the amino group of the side chain of Asn89 interacts with an oxygen atom of the sulphate group in NF023. The side chain of His67 stacks on a naphthalene ring of NF023. Finally, the oxygen atom of the main chain of Cys66 establishes hydrogen bonds with the two –NH groups in the center of NF023 molecule. Concluding, the presence of NF023 is compatible with the crystal packing but the binding event does not seem to be specific enough to impair the dimerization of BIR1. Furthermore, is not possible to conclude whether in the structure obtained NF023 drives XIAP-BIR1 shift or not. Nevertheless, it cannot be excluded that the putative NF023-dependent shift of one BIR molecule relative to the other could impair TAB1 activation as well. All these hypothesis need to be verified *in vitro*, to test TAB1 and TAK1 downstream activation.

4. Production of TRAF2 and cIAP1 as crucial components of TNF-RSC for structural characterization.

TRAFs are important adaptor proteins assembled together with a variety of cellular partners to TNF-RSC, after TNFα-dependent stimulation. In particular, the heterotrimer composed of TRAF1 and two copies of TRAF2 is often reported as a biological platform recruiting crucial components of signaling cascades. TRAFs host RING and Zinc fingers endowed with E3 ligase activity and their binding to cIAPs is essential for cIAPs E3 ligase activity as well. It has been shown that TRAF1 is upregulated in response to diverse stimuli, thus modulating TRAF1/2 binding to cIAP1/2 and, furthermore, that TRAF2 alone is able to trimerize and recognize cIAPs by itself [19]. Since in this work TRAF2-mimetics were designed and preliminarily tested versus cIAP2-BIR1, one of the objectives has actually been the over-production of TRAF2 for structural characterization and for testing TRAF2-mimetics in their ability to disrupt cIAP2-BIR1/TRAF2 recognition.

After several expression tests, TRAF2 (residues 1-501) was produced with a N-terminal His-tag in *E. coli* BL21 (DE3) star™ (Invitrogen™), using a plasmid purchased from GENE Copoeia™. The purification protocol, which was optimized during several purification trials, includes affinity, ion-exchange and size exclusion chromatography. High concentrations of DNAse were used in all buffers, since preliminary purification tests showed an A_{260}/A_{280} ratio of about 1.8, suggesting DNA contamination.

DLS measurements confirmed TRAF2 trimerization (see Table1) and its very elongated shape, as indicated by the axial ratio of ~5. Such results were also supported by analytical gel filtration experiments, where the chromatograms show a peak of absorbance at V_E= 12.89 mL,

corresponding to a molecular weight of about 160 kDa. Thermal stability assays were also performed to screen the buffer conditions preferred by the protein. In the final buffer solution [20 mM Tris-HCl pH 8.0, 500 mM NaCl, 10 mM DTT, 2ng/mL DNase] TRAF2 shows a T_M of 54.8 °C, calculated as the average of three independent experiments (Figure 4.1). Further analytical gel filtration runs have been planned to verify TRAF2 recognition of cIAP2-BIR1 also in the presence of TRAF2-mimetics.

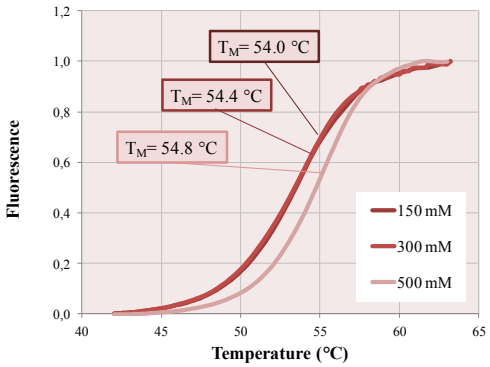

Figure 4.1 Melting curves of TRAF2 tested under different buffer conditions (150, 300 and 500 mM NaCl). The curves reported are obtained from the average of fluorescence values obtained from three independent reads. Melting temperatures are reported into the boxes.

Cellular IAP1 (cIAP1) exists as inactive monomer in the cytoplasm and under TNF-α stimulation acts as a E3 ligase upon dimerization with the homologous cIAP2. In the presence of Smac-mimetics, cIAPs are degraded upon auto-ubiquitylation through a molecular mechanism which remains unknown. For this reason the full length construct of cIAP1 was over-expressed and purified in order to study its biochemical behavior alone and in the presence of the Smac-mimetics from our library. Since in literature nobody over-expressed and purified successfully this protein, in the last year a protocol for cIAP1 production was optimized, to obtain a homogeneous and very pure protein solution to be tested during my structural investigations. To enhance the protein solubility during over-expression in E. coli, cIAP1 was fused with tioredoxin, that favors protein

folding, promoting disulfide bond formation. The sequence of cIAP1 presents, indeed, 24 Cysteine residues, some of which coordinate a zinc ion, and about ten are free to form disulfide bonds. Furthermore, as cIAP1 was frequently subject to proteolysis during the purification process, high salt concentrations (up to 500 mM), a protease inhibitor cocktail (Complete from Roche), and 1 mM of AEBSF, which is a potent non-toxic protease inhibitor, were added into all purification buffers. The protein construct obtained (Trx-cIAP1) was analyzed by DLS (see Table1), analytical gel filtrations and thermal stability assays. The first two techniques revealed that cIAP1 is a quite elongated monomer with a molecular weight of about 100 kDa, as estimated from the elution volume (V_E= 13,36 mL) on Superdex 200 10/300 GL (GE Healthcare). Thermal stability was analyzed in different buffers and in the presence of selected Smac-mimetics (Table 4.1). Two different melting temperatures for each sample were registered, probably due to the progressive unfolding of different domains. The presence of Smac-mimetics generally does not produce a significant shift of T_M values with respect to the apo-protein. NF023 and Suramin cause a minimal shift of the curves to lower temperatures, differing from the major shifts observed for the BIR1 domain curves. Finally, the protein suffers the lack of salt, but stabilization is improved in PBS buffer.

	Trx-cIAP1 (48.3/54.0 ±0. 2°C)		Trx-cIAP1
Smac005	-2.0°C/-1.4°C	**NF023**	-0.3°C/-1.2°C
Smac037	+0.3/+1.9°C	**Suramin**	-0.2°C/-2.3°C
Smac066	-0.4°C/+0.9°C	**No salt**	-4.7°C/-1.3°C
Smac083	+3.9°C/-2.0°C	**PBS 1X**	+3.7°C/-0.6°C

Table 4.1. Melting temperatures (T_M) variations of the protein construct in the presence of Smac-mimetics (left side) and of putative cIAPs-BIR1 inhibitors (right side). Absence of salt and PBS buffer were also tested.

In order to perform new future experiments, such as ubiquitination assays and SAXS experiments for *ab initio* shape determination, the construct was subjected to Trx cleavage, to avoid any impairment of the wild type protein function or conformation. A protocol for the cleavage of tioredoxin was optimized using enterokinase (EK) protease, and screening different temperatures and enzyme concentrations (Figure 4.2).

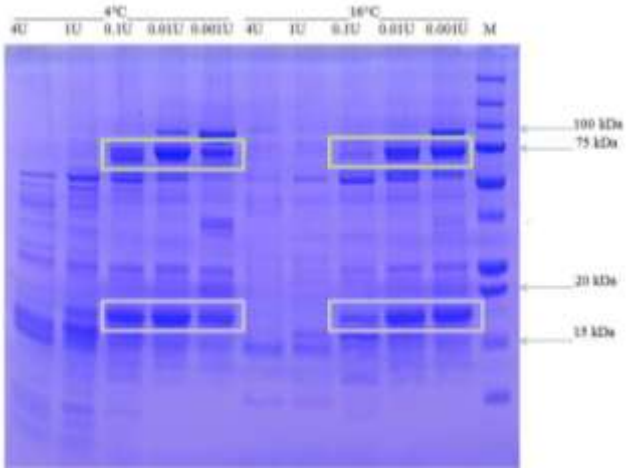

Figure 4.2. SDS-PAGE visualizing the cut trials with EK. M: marker; in each well was loaded a reaction mix containing a different number of unit of enterokinase and 20 µg of protein. The cut generates two segments, one of 17.3 kDa corresponding to thioredoxin (light violet box), and the other one of 70.9 kDa, corresponding to cIAP1 full length (light green box). The immediate upper band is uncut product.

Finally, the cut was performed overnight using 0.05 U of EKMax™ (Invitrogen™) each 20 μg of protein at 4°C with shaking (SDS PAGE data not shown) to perform an efficient cut (absent uncut products) but also to avoid aspecific cut. The protein yield allowed a thermal stability test where the purified wild type cIAP1 displayed a biphasic T_M of 44.4°C and 53.5°C. Further purification and cut experiments have been planned to obtain higher quantity of wild type cIAP1 protein.

Incidentally, the TRAF2 and Trx-cIAP1 constructs were taken to the ESRF Synchrotron in Grenoble for SAXS experiments, which were performed at different protein concentrations (0.5, 1, 2 and 4 mg/ml). In the case of TRAF2, the protein suffered freezing and thawing procedures adopted for transport and resulted proteolysed. Then, it was found that the addition of 1 mM AEBSF stabilizes the protein that remains stable at 4°C for 2-3 weeks, so that after purification the protein can be taken to the Synchrotron. In the case of cIAP1, the SAXS data quality was satisfactory and data analysis is currently in progress by Dr. Mario Milani from the lab.

Conclusions and Future Prospects

In the last three years my PhD experience focused on the study of different proteins and protein domains involved in crucial pathways that drive cells towards life or death. In particular, IAPs and some of their partners were studied as the main targets playing essential roles in the apoptotic cascade. The project started with the development of IAPs-antagonists, known in literature as Smac-mimetics, which have been shown to act as very potent apoptosis inducers in many cancer cell lines presenting IAPs over-expression. The optimization of these small-molecules occurred through a biochemical and structural characterization of their affinity and of their binding modes versus several BIR constructs from homologous IAPs. In detail, Dynamic Light Scattering, analytical size exclusion and thermal stability assays were useful tools to study the hydrodynamic radius, homogeneity and the oligomeric state of the protein samples alone and in the presence of Smac-mimetic compounds, which were tested also for their ability to stabilize the melting temperature of the IAPs constructs here considered. The crystal structures of IAPs-BIR3/Smac-mimetics drove the selection of potent compounds from our library, successfully identifying and optimizing the chemical groups that would improve SM affinity versus cIAP1- and XIAP-BIR3 domains [44; 47; 48] and, therefore, their *in vitro* efficacy. Although the members of the IAP family present high sequence similarity (up to 70%), they developed different mechanisms for inhibiting apoptosis. Interestingly, the structure-based approach described above allowed also to start the development of SM compounds specific for cIAPs or XIAP, with the final aim of studying *in vitro* the different pathways where homologous IAPs are involved. Furthermore, through X-ray crystallography mobile and non-interactive parts of bound Smac-mimetics were identified. These portions have been successfully exploited to

enhance SM bioavailability and to plan the design of divalent compounds, able to simultaneously bind two BIR domains, thus achieving higher potency. Divalent Smac-mimetics binding modes were structurally characterized at high resolution through the analysis of two crystal structures (cIAP1-BIR3/Smac083 and XIAP-BIR3/Smac083), and at low resolution through SAXS experiments on XIAP-BIR23 in the presence of Smac083, where the simultaneous binding was confirmed. Further biochemical and structural experiments are in progress to characterize divalent compounds containing not only different mimic heads but also different heads linkages, which present various flexibility patterns and, interestingly, are now investigated for their influence on Smac-mimetics binding affinity and bioavailability. SAXS, together with analytical gel filtrations and Static Light Scattering experiments performed at the University of Paris-Sud, disclosed important findings on the quaternary structure of Smac/DIABLO and on its binding to XIAP, shedding light, for the first time, on the molecular recognition processes that occurs between these two macromolecules.

Constantly in this work I tried to pay attention to the exponentially growing literature, thus trying to address my research towards unexplored fields of the apoptotic process. In fact, IAPs represents one of the most interesting targets in cancer research; in fact, in the last two years many laboratories committed themselves to the characterization of IAPs and their partners. In particular, the physiological roles of cIAPs have been deeply investigated and defined, while knowledge on the BIR1 domains of homologous IAPs has been further focussed to outline their anti-apoptotic role. As already mentioned, XIAP-BIR1 domain dimerizes and recruits TAB1, to form a macromolecular complex (PDB id: 2POP) for TAK1 recognition, and TAK1-dependent downstream activation of the survival

NF-κB pathway. Analogously, cIAP2-BIR1 is reported to modulate cIAP1/2 recruitment to TNF-RSC through binding to the heterotrimer TRAF1/TRAF2 (PDB id: 3M0D); this binding event is essential for E3 ligase activity of cIAP1/2. Resistance to Smac-mimetics has been observed in some cancer cell lines (*i.e.* small cell lung cancer), where high levels of cIAP2 are detectable even after treatment with SM compounds. The presence of cIAP2 overcomes cIAP1 absence, thus forming a cIAP2/2 complex that maintains anti-apoptotic activity. Furthermore, cIAP2 participates in a positive feedback mechanism, promoting its own expression. For all these reasons, the study of therapies supporting Smac-mimetics have been addressed, consisting in the impairment of XIAP-BIR1/TAB1 and cIAP2/TRAFs recognition events. *In silico* approaches have been used to start the design of TAB1- and TRAF2-mimetics, including (1) the virtual screening of a library of pharmacologically active compounds (LOPAC) versus the cIAP2-BIR1 domain, and (2) a *de novo* design by Dr. Mario Milani (from lab I'm working in) of mimetics based on the TRAF2 residues involved in the interaction with cIAP2-BIR1. These two approaches allowed the identification of NF023, already known as antagonist of the P2X1 receptor and used in humans as vasoconstrictor, and of PEP1 and PEP2, which are predicted to bind cIAP2-BIR1 with nanomolar affinities. NF023 was then *in silico* tested on XIAP-BIR1 and a virtual docking simulation revealed its putative ability to impair both XIAP-BIR1 dimerization and XIAP-BIR1/TAB1 recognition. Suramin, a parental analogue of NF023 was also considered as control in this study, since it is shown to be active as anti-angiogenetic. Furthermore, the dimerization surface of XIAP-BIR1 is homologous to the portion of BIR3 which binds Smac-mimetics, which were then considered for biochemical and structural experiments. Biochemical characterization of the BIR1 domains alone and in the presence of the compounds proposed as

inhibitors (NF023, suramin, PEP1, PEP2 and some of the Smac-mimetics from our library) revealed that generally all the compounds do not affect BIR1 domains stabilization, apart from NF023 and Suramin that heavily decrease the BIR1 melting temperatures. Crystals of cIAP2-BIR1 in the presence of the proposed inhibitors did not present good diffraction patterns and optimization of the crystallization conditions is in progress. The X-ray structures of XIAP-BIR1 and XIAP-BIR1/NF023 did not confirm the positioning of NF023 in the sites predicted by virtual docking probably because NF023 is not able to disrupt the XIAP-BIR1 dimer, but a slight shift of one BIR1 molecule relative to the other was observed in the structure of XIAP-BIR1 in complex with NF023. Should the observed shift be NF023-dependent, further *in vitro* tests will be necessary to verify the impairment of XIAP/TAB1 complex formation and TAK1 activation. Crystallization trials and optimization of crystallization conditions are in progress for the BIR1 domains in the presence of PEP1, PEP2 and SM compounds. In parallel, the design of novel putative TAB1- and TRAF2-mimetics is at the planning stage.

Finally, the over-expression of the full length constructs of two important proteins, TRAF2 and cIAP1 was carried out. Since nobody over-expressed and isolate these proteins earlier with success, the optimization of expression and purification protocols was necessary, due to serious problems concerning proteins solubility and stability. On one hand, the study of TRAF2 binding to cIAP2-BIR1 alone and in the presence of the inhibitors proposed is now in progress, as well as, on the other hand, the analysis of cIAP1 biochemical behavior alone and upon binding to Smac-mimetics. Preliminary SAXS experiments have been performed for the *ab initio* determination of TRAF2 and cIAP1 low resolution structures. Since data quality in the case of TRAF2 was unsatisfactory due to protein

instability issues, SAXS experiments will be repeated with a stabilized protein sample. SAXS data related to cIAP1 are now under analysis by Dr. Mario Milani in collaboration with Dr. Patrice Vachette form the University of Paris-Sud.

Acknowledgments

All the crystals were tested at ESRF in Grenoble (France) at beam lines ID-14 and ID-23. SAXS experiments were carried out at ESRF in Grenoble and at SOLEIL in Gyf-sur-Yvette (Paris – France) thanks to the collaboration of Dr. Patrice Vachette (CNRS-Universite Paris-sud, Orsay, France) and of Dr. Javier Perèz, principal scientist at the beamline SWING in SOLEIL.

References

1. Steller, H. (1995). Mechanisms and genes of cellular suicide. *Science* **267**, 1445-9.
2. Opferman, J. T. & Korsmeyer, S. J. (2003). Apoptosis in the development and maintenance of the immune system. *Nat Immunol* **4**, 410-5.
3. Deveraux, Q. L. & Reed, J. C. (1999). IAP family proteins--suppressors of apoptosis. *Genes Dev* **13**, 239-52.
4. LaCasse, E. C., Baird, S., Korneluk, R. G. & MacKenzie, A. E. (1998). The inhibitors of apoptosis (IAPs) and their emerging role in cancer. *Oncogene* **17**, 3247-59.
5. Vischioni, B., van der Valk, P., Span, S. W., Kruyt, F. A., Rodriguez, J. A. & Giaccone, G. (2006). Expression and localization of inhibitor of apoptosis proteins in normal human tissues. *Hum Pathol* **37**, 78-86.
6. Gyrd-Hansen, M., Darding, M., Miasari, M., Santoro, M. M., Zender, L., Xue, W., Tenev, T., da Fonseca, P. C., Zvelebil, M., Bujnicki, J. M., Lowe, S., Silke, J. & Meier, P. (2008). IAPs contain an evolutionarily conserved ubiquitin-binding domain that regulates NF-kappaB as well as cell survival and oncogenesis. *Nat Cell Biol* **10**, 1309-17.
7. Rajalingam, K. & Dikic, I. (2009). Inhibitors of apoptosis catch ubiquitin. *Biochem J* **417**, e1-3.
8. Schile, A. J., Garcia-Fernandez, M. & Steller, H. (2008). Regulation of apoptosis by XIAP ubiquitin-ligase activity. *Genes Dev* **22**, 2256-66.
9. Lopez, J., John, S. W., Tenev, T., Rautureau, G. J., Hinds, M. G., Francalanci, F., Wilson, R., Broemer, M., Santoro, M. M., Day, C. L. & Meier, P. CARD-mediated autoinhibition of cIAP1's E3 ligase activity suppresses cell proliferation and migration. *Mol Cell* **42**, 569-83.

10. Riedl, S. J., Renatus, M., Schwarzenbacher, R., Zhou, Q., Sun, C., Fesik, S. W., Liddington, R. C. & Salvesen, G. S. (2001). Structural basis for the inhibition of caspase-3 by XIAP. *Cell* **104**, 791-800.

11. Chai, J., Shiozaki, E., Srinivasula, S. M., Wu, Q., Datta, P., Alnemri, E. S. & Shi, Y. (2001). Structural basis of caspase-7 inhibition by XIAP. *Cell* **104**, 769-80.

12. Shiozaki, E. N., Chai, J., Rigotti, D. J., Riedl, S. J., Li, P., Srinivasula, S. M., Alnemri, E. S., Fairman, R. & Shi, Y. (2003). Mechanism of XIAP-mediated inhibition of caspase-9. *Mol Cell* **11**, 519-27.

13. Lu, M., Lin, S. C., Huang, Y., Kang, Y. J., Rich, R., Lo, Y. C., Myszka, D., Han, J. & Wu, H. (2007). XIAP induces NF-kappaB activation via the BIR1/TAB1 interaction and BIR1 dimerization. *Mol Cell* **26**, 689-702.

14. Liu, J., Zhang, D., Luo, W., Yu, Y., Yu, J., Li, J., Zhang, X., Zhang, B., Chen, J., Wu, X. R., Rosas-Acosta, G. & Huang, C. X-linked inhibitor of apoptosis protein (XIAP) mediates cancer cell motility via Rho GDP dissociation inhibitor (RhoGDI)-dependent regulation of the cytoskeleton. *J Biol Chem* **286**, 15630-40.

15. Crook, N. E., Clem, R. J. & Miller, L. K. (1993). An apoptosis-inhibiting baculovirus gene with a zinc finger-like motif. *J Virol* **67**, 2168-74.

16. Hui, S. K., Tse, M. K., Yang, Y., Wong, B. C. & Sze, K. H. Backbone and side-chain 1H, 13C and 15N assignments of the ubiquitin-associated domain of human X-linked inhibitor of apoptosis protein. *Biomol NMR Assign* **4**, 13-5.

17. Mace, P. D., Linke, K., Feltham, R., Schumacher, F. R., Smith, C. A., Vaux, D. L., Silke, J. & Day, C. L. (2008). Structures of the cIAP2 RING domain reveal conformational changes associated with ubiquitin-conjugating enzyme (E2) recruitment. *J Biol Chem* **283**, 31633-40.

18. LaCasse, E. C., Mahoney, D. J., Cheung, H. H., Plenchette, S., Baird, S. & Korneluk, R. G. (2008). IAP-targeted therapies for cancer. *Oncogene* **27**, 6252-75.

19. Zheng, C., Kabaleeswaran, V., Wang, Y., Cheng, G. & Wu, H. Crystal structures of the TRAF2: cIAP2 and the TRAF1: TRAF2: cIAP2 complexes: affinity, specificity, and regulation. *Mol Cell* **38**, 101-13.

20. Petersen, S. L., Wang, L., Yalcin-Chin, A., Li, L., Peyton, M., Minna, J., Harran, P. & Wang, X. (2007). Autocrine TNFalpha signaling renders human cancer cells susceptible to Smac-mimetic-induced apoptosis. *Cancer Cell* **12**, 445-56.

21. Varfolomeev, E., Blankenship, J. W., Wayson, S. M., Fedorova, A. V., Kayagaki, N., Garg, P., Zobel, K., Dynek, J. N., Elliott, L. O., Wallweber, H. J., Flygare, J. A., Fairbrother, W. J., Deshayes, K., Dixit, V. M. & Vucic, D. (2007). IAP antagonists induce autoubiquitination of c-IAPs, NF-kappaB activation, and TNFalpha-dependent apoptosis. *Cell* **131**, 669-81.

22. Vince, J. E., Wong, W. W., Khan, N., Feltham, R., Chau, D., Ahmed, A. U., Benetatos, C. A., Chunduru, S. K., Condon, S. M., McKinlay, M., Brink, R., Leverkus, M., Tergaonkar, V., Schneider, P., Callus, B. A., Koentgen, F., Vaux, D. L. & Silke, J. (2007). IAP antagonists target cIAP1 to induce TNFalpha-dependent apoptosis. *Cell* **131**, 682-93.

23. Kim, J. Y., Morgan, M., Kim, D. G., Lee, J. Y., Bai, L., Lin, Y., Liu, Z. G. & Kim, Y. S. TNFalpha induced noncanonical NF-kappaB activation is attenuated by RIP1 through stabilization of TRAF2. *J Cell Sci* **124**, 647-56.

24. Bertrand, M. J. & Vandenabeele, P. The Ripoptosome: death decision in the cytosol. *Mol Cell* **43**, 323-5.

25. Feoktistova, M., Geserick, P., Kellert, B., Dimitrova, D. P., Langlais, C., Hupe, M., Cain, K., MacFarlane, M., Hacker, G. & Leverkus, M. cIAPs block Ripoptosome formation, a RIP1/caspase-8 containing intracellular cell death complex differentially regulated by cFLIP isoforms. *Mol Cell* **43**, 449-63.

26. Tenev, T., Bianchi, K., Darding, M., Broemer, M., Langlais, C., Wallberg, F., Zachariou, A., Lopez, J., MacFarlane, M., Cain, K. & Meier, P. The Ripoptosome, a signaling platform that assembles in response to genotoxic stress and loss of IAPs. *Mol Cell* **43**, 432-48.

27. Du, C., Fang, M., Li, Y., Li, L. & Wang, X. (2000). Smac, a mitochondrial protein that promotes cytochrome c-dependent caspase activation by eliminating IAP inhibition. *Cell* **102**, 33-42.

28. Verhagen, A. M., Ekert, P. G., Pakusch, M., Silke, J., Connolly, L. M., Reid, G. E., Moritz, R. L., Simpson, R. J. & Vaux, D. L. (2000). Identification of DIABLO, a mammalian protein that promotes apoptosis by binding to and antagonizing IAP proteins. *Cell* **102**, 43-53.

29. Liu, Z., Sun, C., Olejniczak, E. T., Meadows, R. P., Betz, S. F., Oost, T., Herrmann, J., Wu, J. C. & Fesik, S. W. (2000). Structural basis for binding of Smac/DIABLO to the XIAP BIR3 domain. *Nature* **408**, 1004-8.

30. Wu, G., Chai, J., Suber, T. L., Wu, J. W., Du, C., Wang, X. & Shi, Y. (2000). Structural basis of IAP recognition by Smac/DIABLO. *Nature* **408**, 1008-12.

31. Ekert, P. G., Silke, J., Hawkins, C. J., Verhagen, A. M. & Vaux, D. L. (2001). DIABLO promotes apoptosis by removing MIHA/XIAP from processed caspase 9. *J Cell Biol* **152**, 483-90.

32. Srinivasula, S. M., Hegde, R., Saleh, A., Datta, P., Shiozaki, E., Chai, J., Lee, R. A., Robbins, P. D., Fernandes-Alnemri, T., Shi, Y. & Alnemri, E. S. (2001). A conserved XIAP-interaction motif in caspase-9 and Smac/DIABLO regulates caspase activity and apoptosis. *Nature* **410**, 112-6.

33. Chai, J., Du, C., Wu, J. W., Kyin, S., Wang, X. & Shi, Y. (2000). Structural and biochemical basis of apoptotic activation by Smac/DIABLO. *Nature* **406**, 855-62.

34. Kulathila, R., Vash, B., Sage, D., Cornell-Kennon, S., Wright, K., Koehn, J., Stams, T., Clark, K. & Price, A. (2009). The structure of the BIR3 domain of cIAP1 in complex with the N-terminal peptides of SMAC and caspase-9. *Acta Crystallogr D Biol Crystallogr* **65**, 58-66.

35. Nikolovska-Coleska, Z., Meagher, J. L., Jiang, S., Kawamoto, S. A., Gao, W., Yi, H., Qin, D., Roller, P. P., Stuckey, J. A. & Wang, S. (2008). Design and characterization of bivalent Smac-based peptides as antagonists of XIAP and development and validation of a fluorescence polarization assay for XIAP containing both BIR2 and BIR3 domains. *Anal Biochem* **374**, 87-98.

36. Petersen, S. L., Peyton, M., Minna, J. D. & Wang, X. Overcoming cancer cell resistance to Smac mimetic induced apoptosis by modulating cIAP-2 expression. *Proc Natl Acad Sci U S A*.

37. Lecis, D., Drago, C., Manzoni, L., Seneci, P., Scolastico, C., Mastrangelo, E., Bolognesi, M., Anichini, A., Kashkar, H., Walczak, H. & Delia, D. Novel SMAC-mimetics synergistically stimulate melanoma cell death in combination with TRAIL and Bortezomib. *Br J Cancer* **102**, 1707-16.

38. Lu, J., Bai, L., Sun, H., Nikolovska-Coleska, Z., McEachern, D., Qiu, S., Miller, R. S., Yi, H., Shangary, S., Sun, Y., Meagher, J. L., Stuckey, J. A. & Wang, S. (2008). SM-164: a novel, bivalent Smac mimetic that induces apoptosis and tumor regression by concurrent removal of the blockade of cIAP-1/2 and XIAP. *Cancer Res* **68**, 9384-93.

39. Zobel, K., Wang, L., Varfolomeev, E., Franklin, M. C., Elliott, L. O., Wallweber, H. J., Okawa, D. C., Flygare, J. A., Vucic, D., Fairbrother, W. J. & Deshayes, K. (2006). Design, synthesis, and biological activity of a potent Smac mimetic that sensitizes cancer cells to apoptosis by antagonizing IAPs. *ACS Chem Biol* **1**, 525-33.

40. Flygare, J. A. & Fairbrother, W. J. Small-molecule pan-IAP antagonists: a patent review. *Expert Opin Ther Pat* **20**, 251-67.

41. Vucic, D., Deshayes, K., Ackerly, H., Pisabarro, M. T., Kadkhodayan, S., Fairbrother, W. J. & Dixit, V. M. (2002). SMAC negatively regulates the anti-apoptotic activity of melanoma inhibitor of apoptosis (ML-IAP). *J Biol Chem* **277**, 12275-9.

42. Guo, F., Nimmanapalli, R., Paranawithana, S., Wittman, S., Griffin, D., Bali, P., O'Bryan, E., Fumero, C., Wang, H. G. & Bhalla, K. (2002). Ectopic overexpression of second mitochondria-derived activator of caspases (Smac/DIABLO) or cotreatment with N-terminus of Smac/DIABLO peptide potentiates epothilone B derivative-(BMS 247550) and Apo-2L/TRAIL-induced apoptosis. *Blood* **99**, 3419-26.

43. Sun, H., Nikolovska-Coleska, Z., Yang, C. Y., Xu, L., Liu, M., Tomita, Y., Pan, H., Yoshioka, Y., Krajewski, K., Roller, P. P. & Wang, S. (2004). Structure-based design of potent, conformationally constrained Smac mimetics. *J Am Chem Soc* **126**, 16686-7.

44. Mastrangelo, E., Cossu, F., Milani, M., Sorrentino, G., Lecis, D., Delia, D., Manzoni, L., Drago, C., Seneci, P., Scolastico, C., Rizzo, V. & Bolognesi, M. (2008). Targeting the X-linked inhibitor of apoptosis protein through 4-substituted azabicyclo[5.3.0]alkane smac mimetics. Structure, activity, and recognition principles. *J Mol Biol* **384**, 673-89.

45. Feltham, R., Bettjeman, B., Budhidarmo, R., Mace, P. D., Shirley, S., Condon, S. M., Chunduru, S. K., McKinlay, M. A., Vaux, D. L., Silke, J. & Day, C. L. Smac mimetics activate the E3 ligase activity of cIAP1 protein by promoting RING domain dimerization. *J Biol Chem* **286**, 17015-28.

46. Li, L., Thomas, R. M., Suzuki, H., De Brabander, J. K., Wang, X. & Harran, P. G. (2004). A small molecule Smac mimic potentiates TRAIL- and TNFalpha-mediated cell death. *Science* **305**, 1471-4.

47. Cossu, F., Mastrangelo, E., Milani, M., Sorrentino, G., Lecis, D., Delia, D., Manzoni, L., Seneci, P., Scolastico, C. & Bolognesi, M. (2009). Designing Smac-mimetics as antagonists of XIAP, cIAP1, and cIAP2. *Biochem Biophys Res Commun* **378**, 162-7.

48. Cossu, F., Malvezzi, F., Canevari, G., Mastrangelo, E., Lecis, D., Delia, D., Seneci, P., Scolastico, C., Bolognesi, M. & Milani, M. Recognition of Smac-mimetic compounds by the BIR domain of cIAP1. *Protein Sci* **19**, 2418-29.

49. Dupeux, F., Rower, M., Seroul, G., Blot, D. & Marquez, J. A. A thermal stability assay can help to estimate the crystallization likelihood of biological samples. *Acta Crystallogr D Biol Crystallogr* **67**, 915-9.

50. Cossu, F., Milani, M., Mastrangelo, E., Vachette, P., Servida, F., Lecis, D., Canevari, G., Delia, D., Drago, C., Rizzo, V., Manzoni, L., Seneci, P., Scolastico, C. & Bolognesi, M. (2009). Structural basis for bivalent Smac-mimetics recognition in the IAP protein family. *J Mol Biol* **392**, 630-44.

51. Koch, M. H., Vachette, P. & Svergun, D. I. (2003). Small-angle scattering: a view on the properties, structures and structural changes of biological macromolecules in solution. *Q Rev Biophys* **36**, 147-227.